Applied Energy 371 (2024) 123666

Contents lists available at ScienceDirect

Applied Energy

journal homepage: www.elsevier.com/locate/apenergy

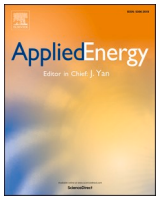

# Community-based transactive energy market concept for 5th generation district heating and cooling through distributed optimization

Qiwei Qin, Louis Gosselin *

*Department of Mechanical Engineering, Université Laval, Quebec City, Quebec, Canada*

## HIGHLIGHTS

- 5th generation district heating and cooling (5GDHC) uses heat sharing among prosumers.
- New distributed optimization of 5GDHC has below 5% difference with central optimizer.
- The new market determines internal price of thermal energy and prosumers' demand.
- 5GDHC generates savings of up to 40% under different electricity tariffs.

## ARTICLE INFO

*Keywords:*
Bidirectional low-temperature district energy system
Demand-side management
Distributed optimization
Jacobi-proximal ADMM
Community-based market

## ABSTRACT

Fifth-generation district heating and cooling (5GDHC) is an emerging concept that exploits heat sharing among prosumers through a low-temperature bidirectional loop. Coordinating the energy interactions in such a system is a complex problem, typically solved through centralized optimization. In addition to privacy issues for prosumers, centralized optimization can prove too hard to solve for large 5GDHC systems and cannot establish a profit distribution between prosumers. To overcome these drawbacks, this paper develops a community-based transactive energy market framework based on distributed optimization of 5GDHC. The optimization is based on the Jacobi-proximal alternating direction method of multipliers. The approach relies on iterative interactions between the network coordinator and the prosumers, the former adjusting the internal price of thermal energy and the latter adapting their heating and cooling demand. A series of test-case 5GDHC networks involving houses, commercial buildings, data centers and central boilers and chillers were numerically simulated to demonstrate how the proposed framework performs, under three electricity tariff structures (constant, time-of-use or pay for peak). Results show that, for the cases tested, the gap between the proposed approach and global optimization is below 5% and that electricity savings compared to a situation without 5GDHC could reach 40%. The proposed method allowed to dynamically adjust the internal price of thermal energy and the prosumers' demand while considering their thermal dissatisfaction. By facilitating 5GDHC operation, this work could help their practical implementation in the future.

## 1. Introduction

### 1.1. Context

District heating and cooling systems (DHC) are crucial for achieving an emission-free supply of heating and cooling. The evolution of district heating is often divided into five generations. Although such a classification is not perfect, it can help to understand the advances in district heating. The latest stage in the development of DHC systems is the *5th Generation District Heating and Cooling* (5GDHC) networks [1], which are also referred to as *Bidirectional Low-Temperature Networks* [2] or *Cold District Heating Networks* [3]. Consumers in 5GDHC are connected to a single loop consisting of one warm and one cold pipe (two-pipe system). Since the temperatures of both lines are close to the ambient (e.g., between 5 and 30 °C), decentralized heat pumps are necessary to bridge the temperature gap between the network and the requirements of different consumers. Differently, in the previous generations, two dedicated loops would be needed (four-pipe system), i.e. one for cooling and one for heating [4]. In the 4th generation networks, the focus is on improving the (central) supply side, for example, through the integration of renewable energy sources and recovery from external waste heat

* Corresponding author.
*E-mail address:* Louis.Gosselin@gmc.ulaval.ca (L. Gosselin).

https://doi.org/10.1016/j.apenergy.2024.123666
Received 10 July 2023; Received in revised form 5 May 2024; Accepted 6 June 2024

**Nomenclature**

| | |
|---|---|
| $c_E$ | electricity price for peak, \$ kW$^{-1}$ |
| $C_i$ | thermal capacitance of node i, J K$^{-1}$ |
| $COP_C$ | Coefficient of performance in cooling mode |
| $COP_H$ | Coefficient of performance in heating mode |
| $\dot{D}_s$ | rate of electricity consumption of servers, W |
| $\dot{E}_i$ | total rate of electricity consumption of a node i, W |
| $\dot{E}_D$ | total rate of electricity consumption of data center, W |
| $\dot{E}_{in,i}$ | rate of electricity consumption for node's I internal load, W |
| $J$ | objective function, \$ |
| $M$ | large number |
| $N$ | number of buildings |
| $p_E$ | real-time electricity price, \$ kWh$^{-1}$ |
| $\dot{Q}_{Boiler}$ | heat production of boiler, W |
| $\dot{Q}_{Chiller}$ | heat extraction of chiller, W |
| $\dot{Q}_{in,i}$ | thermal demand of a node i, W |
| $\dot{Q}_{gain,i}$ | heat gains at a node i, W |
| $\dot{Q}_{net,i}$ | heat exchange of a node i with the network, W |
| $\dot{Q}_{net,Central}$ | net heat demand from central plant, W |
| $R_i$ | thermal resistance of node i, m K$^{-1}$ |
| $t$ | time, h |
| $T_{am}$ | ambient temperature, K |
| $T_{in,i}$ | indoor temperature of node i, K |
| $u_D$ | coefficient, \$/kWh$^2$ |
| $U_D$ | unsatisfaction function of data center, \$ |
| $u_i$ | coefficient, \$ person$^{-1}$ K$^{-2}$ |
| $U_i$ | unsatisfaction function of bode I, \$ |
| z | auxiliary variable |

*Greek symbols*

| | |
|---|---|
| $\alpha$ | auxiliary binary variable |
| $\eta_{Boiler}$ | efficiency of boiler |
| $\lambda$ | dual variable (internal price of thermal energy), \$/W |
| $\pi_i$ | amount received or paid by node i, \$ |
| $\omega_i$ | occupancy of node i, persons |

*Abbreviations*

| | |
|---|---|
| ADMM | alternating direction method of multipliers |
| DHC | district heating and cooling |
| HP | heat pump |
| MIQP | mixed integer quadratic programming |
| PJ-ADMM | Proximal-Jacobian ADMM |
| 5GDHC | 5th generation district heating and cooling |

sources. On the other hand, in the 5th generation networks, the motivation is to exploit exchanges of heat and cold between participants, redefining the supply-demand relationships and the money flows in the network. Consumers become prosumers and can contribute to satisfying the thermal demands of others. Real cases of 5GDHC have been documented in [5].

### 1.2. Main features of 5GDHC

5GDHC is a relatively new concept, although some of the ideas on which it relies have been studied in the past. A query in Web of Science with keywords such as "5GDHC", "bidirectional networks" or ("fifth generation" AND "district heating") returned only 50 publications (after removing papers not related with the 5GDHC concept, as of June 2023), most of which having been published in the last 3 years. These papers focus on developing design and operation guidelines, techno-economic studies, and simulation (and co-simulation) models. However, as will be described below, several other aspects, such as market mechanisms, have received little attention so far.

One of the advantages of 5GDHC is that for districts with simultaneous heating and cooling demands, a portion of the thermal needs can be balanced out by the bidirectional low-temperature networks. Compared with traditional district heating and cooling networks that supply heating and cooling separately, 5GDHC can recover waste heat from the cooling demand side. Consequently, the installed capacity of supply units such as boilers or chillers can be reduced. Differently from consumers in traditional district energy systems, a prosumer in 5GDHC is an active player that can consume, but also produce energy [6]. Prosumers in DHC grids can produce thermal energy, draw thermal energy from the network or reject excess heat to the network when needed [7].

The potential of 5GDHC for reducing the cost and environmental footprint of heating and cooling in the building sector has been demonstrated in several studies [2,8]. However, the optimal operation of 5GDHC is known to be a challenging task due to its high complexity. For example, in 5GDHC, the heat demand of a prosumer can be satisfied by the central heating plant, the cooling demand of other prosumers, or low-grade heat sources such as geothermal or solar energy. Optimally balancing the decentralized thermal supply and demand in real-time for the whole district is computationally intensive [9].

In addition to the problem of balancing energy supply and demand, the coordination of different building thermal demands can be another challenge in the operation of 5GDHC. Buildings can function like thermal storage by allowing the indoor temperature to float between an upper and a lower bound, given an adequate range of thermal comfort. In other words, the thermal demand of different types of buildings can be considered as thermostatically controlled loads. Demand flexibility can be leveraged for load management or demand response [10]. However, such flexibility complexifies the balancing problem mentioned above. 5GDHC benefits from smart energy management systems and, in such cases, can be qualified of smart thermal grids [11]. Such systems should be able to schedule and manage the energy flows between different components of the 5GDHC network to fully exploit synergies and performance curves between thermal storage, thermostatically controlled loads and equipment.

### 1.3. Optimization of energy management in thermal grids

In that context, optimization-based energy management can be a good tool for operating 5GDHC. Optimal power flow or optimal energy flow problems are not new in electricity or thermal energy systems [12,13]. Linear Programming, Mixed Integer Linear Programming, Non-Linear Programming, Mixed Integer Non-Linear Programming as well as some evolutionary algorithms such as Genetic Algorithm or Particle Swarm Optimization are used to optimize design or operation of district thermal energy systems [14]. Generally, the operation of the energy system is formulated as a global optimization problem with one or several objective functions for the whole system, as well as constraints and a set of decision variables. Then, a central solver gathers all the required information for solving the optimization problem, such as the features of the appliances of the prosumers, the occupancy profiles, etc. According to this information, the optimal operation over a certain time horizon of all the devices connected to the district can be determined. Although this theoretical centralized or ubiquitous optimization-based energy management appears to be straightforward to implement, it comes with major drawbacks. The first one is the privacy protection of the participants, as a centralized solver needs detailed information and direct control of the participants' appliances. A second issue is that when

minimizing the objective function for the whole district, the centralized optimization cannot distinguish the "profit distribution" between prosumers. In other words, the optimal action for the whole district may not be the optimal action for some participants. A third inconvenience is that this approach will eventually face "the curse of dimensionality". This means that the optimization may become computationally infeasible when the number of decision variables is large, which is typically the case in real district energy systems.

Hence, recent research [15,16] developed game-theory based models or decentralized solution methods to formulate more realistic scenarios for the operation of distributed energy management systems. The basic idea of distributed optimization methods is to divide a complex optimization problem into an iteration of several sub-problems (blocks) that are easier to solve. The sub-problems are solved in parallel at each iteration when a specific coordination is needed to satisfy global constraints until a convergence criterion is met. The global constraints are usually related to the physical relationship of energy flows in the energy management systems [17]. Distributed algorithms based on the alternating direction method of multipliers (ADMM) are often used in energy management systems. ADMM were developed to solve convex optimization problems with equality constraints with a very large number of variables, as detailed in a recent review on the topic [18]. For multi-block ADMM, there are three fundamental types: Variable Splitting ADMM, Gauss-Seidel ADMM, and Jacobian ADMM [19]. One of the major drawbacks of the above methods are that these algorithms may diverge for multi-node problems. A variation called Proximal-Jacobian ADMM (PJ-ADMM) was derived in [19] to avoid divergence.

For convex problems, dual decomposition methods such as ADMM converge to the optimal global solution. Otherwise, there is a duality gap between the centralized and distributed optimization solutions. ADMM can still be used if the duality gap is small. Distributed algorithms based on ADMM are used in electricity networks [20,21]. However, few studies on distributed optimization for thermal grids were found. As reported by Ref. [22], the existing literature currently lacks a distributed optimization mechanism for buildings connected to a district heating and cooling system, and this is particularly true for 5GDHC systems.

### 1.4. Profit distributions and market mechanisms

Any 5GDHC operation optimization problem such as the one investigated here requires a reasonable and clear profit distribution rule (consumer-centric market mechanisms) [23]. Prosumers may be more interested in their personal profit rather than that of the whole district, and it is known that tariffs can motivate consumers to adjust their demand. For example, a tariff to encourage consumers to lower their return temperature in the framework of 4GDH was proposed in [24]. Literature states that an ideal market mechanism should aim for four properties, but unfortunately, no market can fully achieve the four properties at the same time [23]. First, an efficient market should ensure that prosumers are satisfied with the outcomes of the proposed mechanisms while ensuring a maximal profit. Such property of a market is called efficiency [25]. Compared to centralized optimization, distributed optimization can potentially help define a payment rule that maximizes individual benefits for each prosumer as well as overall benefits. Second, a mechanism is said to be incentive-compatible if every participant can achieve the best outcome for themselves just by acting according to their true preferences [25], i.e. lying or cheating do not help the participants to increase their benefits. Third, another property of the market mechanisms is its budget balance. A strongly-budget-balanced mechanism is a mechanism in which the sum of the payments made by the participants and received by them is exactly 0. This means that all money exchanges are made among the participants [26]. Finally, the property of individual rationality means that no participant can benefit from splitting apart from the community.

Under the framework of 5GDHC, users become prosumers and can exchange heat or cold through a single loop, creating a unique synergetic system. In previous generations, heating providers have always been on the supply side, which means that the cash flow is from heated buildings to the supply side. However, in 5GDHC, buildings with a heating demand can be seen as the supply side of buildings with a cooling demand, and vice versa. Therefore, the cash flow between the stakeholders should be further clarified. The questions of how to effectively generate benefits from these strong heat interactions and how to share profits in such a system are still not understood. Mastering these topics is vital for the deployment of 5GDHC and, in the end, to materialize its economic and environmental benefits.

### 1.5. Gap in literature and contributions of the paper

Different gaps in current literature were noted above. Two of the main gaps can be summarized as:

- As revealed by the above literature review, there is currently a lack of distributed optimization strategies for 5th generation district heating and cooling systems. Although distributed optimization approaches have been developed and applied to electric grids, their adaptation to and use for 5GDCH (i.e., smart thermal grids) needs some attention. Due to the inherent features (simultaneous heating and cooling demands, with sharing of cold and heat between prosumers) and original configurations (shared two-pipe low temperature loop, booster heat pumps, etc.) of 5GDHC, distributed optimization needs to be adapted, tested, and assessed.
- The new paradigm behind 5GDHC is that the heat that one prosumer rejects in the loop can be beneficial to another prosumer who needs it, and inversely, we can say that the fact that one prosumer accepts to remove heat from the loop to satisfy its own heating need is helpful to the prosumer who needs to reject heat to satisfy its cooling demand. The problem becomes even more complex when considering that prosumers can also adjust their thermal demands to help balance the 5GDHC network. In such a system, the distribution of benefits and the market mechanisms are not well understood.

The first novelty of the present paper is thus to introduce, develop and assess a transactive distributed energy management strategy for 5GDHC systems. As highlighted in the first gap above, distributed optimization for 5GDHC, and in particular with PJ-ADMM, has received little interest so far. The second novelty of this work consists in the development of benefit distribution rules and market mechanisms for 5GDHC with active prosumers that can adjust their demand depending on the thermal energy cost, an important topic that has not been studied thoroughly in 5GDHC (see gap 2 above). In the paper, a benefit allocation rule was established based on the Proximal-Jacobian ADMM and the properties of the resulting profit distribution mechanism were studied. The effectiveness and scalability of the proposed distributed optimization were tested with different test cases. It was found that the proposed framework was successful in dynamically adapting the internal price of thermal energy and the prosumers' demands under different electricity tariff structures and that this resulted in energy and cost savings.

### 1.6. Organization of the paper

The organization of this article is as follows: Section 2 introduces the modeling of the different system components, unsatisfaction function, and local and global constraints of 5th generation district heating and cooling systems under study. Section 3 presents the centralized and distributed optimization algorithms that will be compared. Based on distributed optimization, an energy market concept for profit distribution is defined. Section 4 analyzes the four properties of the proposed mechanism. Section 5 validates the effectiveness, scalability of the distributed optimization, and the motivations of the coordinator and prosumers in different districts under different electricity rates. Section

6 presents the conclusion and future work.

## 2. Modeling of heat and electricity balances and unsatisfaction

Our study aims at determining the optimal energy management of a district with a bidirectional low-temperature network. To do that, a sub-model of each of the main components of the system is required. These sub-models will take the form of heat balances and electricity balances that will be used as constraints in the optimization models introduced later in Section 3. The present section explains each of these sub-models. First, the configuration of the test case DHC system is introduced in Section 2.1. Then, the electricity and heat balances of buildings, data centers and central plants are presented in Sections 2.2 to 2.4. Finally, Section 2.5 explains how the unsatisfaction of each prosumer was determined as a function of how much they had to adapt their demand.

### 2.1. 5GDHC test-case system

To apply the framework developed in this work, a 5GDHC system was elaborated and is illustrated in Fig. 1. Note that the framework proposed in this work could easily be extended to other districts as well. The test-case community consists of different types of buildings (households and commercial buildings) and one data center. Each prosumer is connected to the cold and warm loops, allowing them to extract or reject heat depending on their demand at that particular moment. A heat pump is used to bridge the temperature gap between the network and the temperature requirement of the end users. Table 1 summarizes the main features of the different prosumers. Furthermore, a central plant operated by a "network coordinator" compensates for the imbalance between the different heating and cooling needs of the prosumers. This is accomplished with central boilers and chillers.

For developing the models, different assumptions were made. Regarding the central plant, the chillers and boilers are used to balance the network. We assumed that electrical boilers were used with a constant efficiency of 95%. This equipment was selected since the outdoor design temperature in Quebec is too low to allow central heat pumps to balance the network. Furthermore, since electricity in Quebec is

**Table 1**
Summary of the main features of different nodes of the 5GDHC system.

| Node type | Description | Demand | Modeling method |
|---|---|---|---|
| Building nodes | Single-family detached house | Heating or cooling demand to meet occupants' comfort | Section 2.2 |
| | Medium office building | Heating or cooling demand to meet occupants' comfort | Section 2.2 |
| Data center node | Data center | Cooling demand caused by computers | Section 2.3 |
| Central plant node | Boilers and chillers | | Section 2.4 |

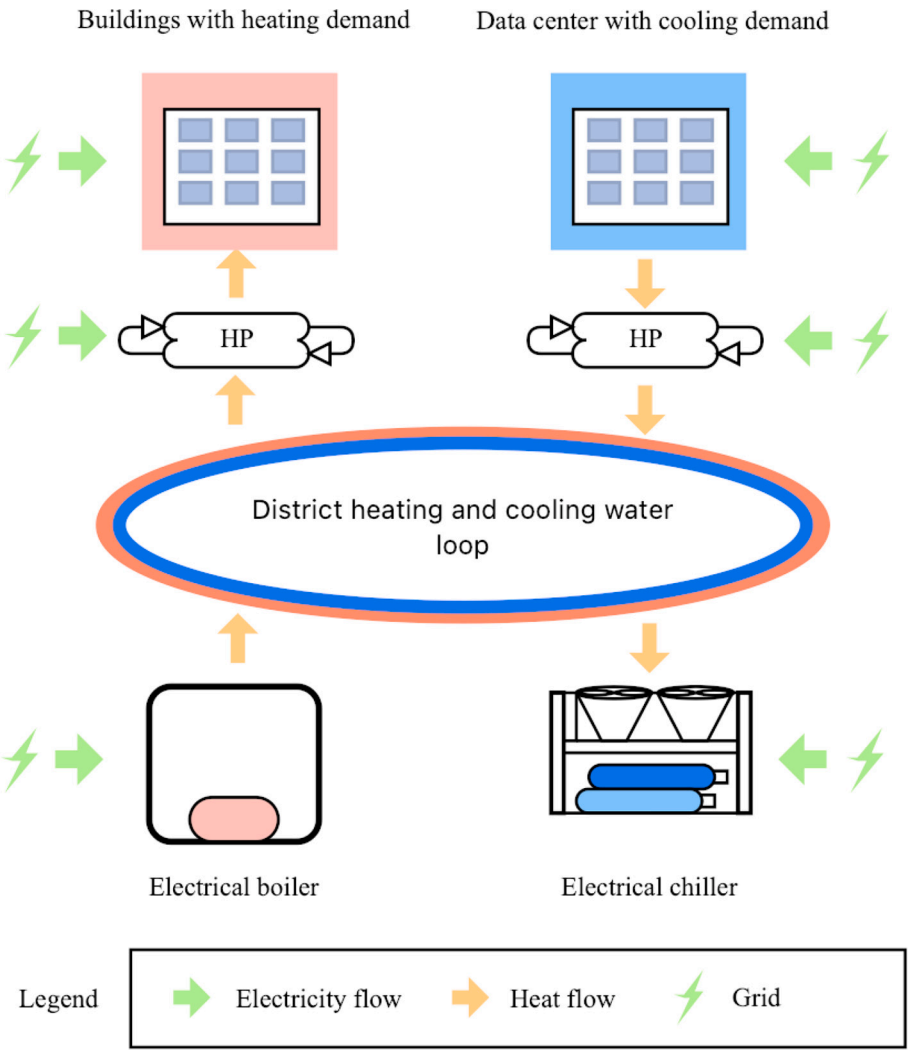


**Fig. 1.** Schematic representation of the test case district energy system studied in this work.

typically from renewable sources and is relatively cheap, electric systems for space-heating are often used. Similarly, the COP of the chillers was constant and fixed at 3.5. Even though the COP would typically vary over time due to changes in temperature, this effect was not considered since only 24-h simulations were carried out, and over such a short period, variations of COP are much smaller. As for the warm and cold loops, their thermos-fluid features were not simulated explicitly, as the focus of the present work is on market mechanisms and energy and cash flows between prosumers. This approach eliminates the need to specify the layout and detailed characteristics of the system (e.g., pipe diameter, etc.). No heat loss or thermal inertia is considered. This modeling of the system was found to be adequate for the purpose of this study (especially since it is used for operational optimization, which could be time-consuming). Future work could easily relax these simplifying assumptions in the proposed framework.

The COP of the heat pumps of the prosumers depends on the temperature level of the network and the temperature requirement of the demand side. The temperature level of the network in this article is assumed to be ~20 °C [1]. A constant COP value of 3 for the heat pump in the heating mode was determined based on [27] assuming that the temperature requirement on the heating demand side was ~50 °C [28]. For the cooling mode, a COP value of 5.6 was considered, assuming a temperature requirement of the cooling demand side of ~10 °C [29,30]. Note that the different temperature values mentioned above were used solely for selecting appropriate equipment and their efficiencies. Since the thermo-fluid features of the network were not explicitly simulated, these temperatures do not intervene directly in the present model. For example, the specified temperature level of the network (i.e., ~20 °C) represents a characteristic temperature of both the cold and warm pipes, as the present operational model does not require specifying the temperature difference between both pipes. As can be seen, in the present study, the efficiency of the end-users' heat pump is higher than that of the central plant, which means that, whenever possible, it is best to rely on heat exchanges between prosumers rather than on generating heat and cold centrally.

Finally, the last simplifying assumption of the model consists in neglecting pumping power. Previous work in a similar system showed that pumping represented <2% of thermal loads for 5GDHC [31]. However, it is important to recognize that depending on the system characteristics, the mass flow rate in the cold and warm pipes can be large when the temperature difference between both loops is small. Nevertheless, in the present case, since the thermal loads are managed by the central plant with electricity-driven boilers and chillers, the plant's electrical loads are expected to be dominated by heating and cooling. Pumping power does not affect the structure of the proposed framework but could be added in future work to better estimate costs. Accounting for it would require designing the details of the loop (pipe diameters, layout, etc.), which was not the purpose of this work.

For the sake of comparison, it is also possible to define a scenario in which the 5GDHC system would not be used. In that case, each consumer would simply operate their own boiler and chiller, and no heat exchanges between them would be allowed. This will serve as a reference later for establishing the benefits of the 5GDHC system.

It is important to mention that, as can be seen in Fig. 1, the only external source of energy for the case-study network is electricity. One of the reasons for this choice is based on the local energy context in the province of Quebec (Canada), where 99% of the electricity is from renewable sources, motivating the electrification of the heating and cooling systems. When comparing the proposed 5GDHC with a situation in which each building would satisfy its demand with its own boiler and chiller (called "reference" in the previous paragraph), the comparison in terms of primary energy is straightforward and transparent. In other contexts, although the proposed optimization framework would still apply, further analysis might be needed to compare the system to a reference in which fuel could be used.

### 2.2. Building thermal dynamic model

Space cooling and heating demands are thermostatically controlled loads [10]. In this paper, reduced-order models are used to simulate the thermal dynamics of buildings [32]. Each building is modeled as a single zone with a uniform indoor temperature. A first-order linear model (i.e., 1R1C) is used because it can provide a decent simulation accuracy while avoiding the over-fitting risks of higher order models. For the $i^{th}$ building at a given time, the heat transfer balance in the building with a 1R1C model is:

$$C_i \frac{\partial T_{in,i}}{\partial t} = \frac{T_{in,i} - T_{am}}{R_i} + \dot{Q}_{gain,i} + \dot{Q}_{in,i} \tag{1}$$

where $C_i$ and $R_i$ are the thermal capacitance and effective thermal resistance for building i. $T_{in,i}$ is the indoor temperature and $T_{am}$ is the ambient outdoor temperature. $\dot{Q}_{gain,i}$ accounts for the different heat gains (solar gains and internal heat gains from occupancy, lights, and equipment). $\dot{Q}_{in,i}$ is the thermal demand (heating or cooling demand) of the building. In order to simplify the present model, we assumed that each building could only request either heating or cooling from the network at a given time. In other words, if simultaneous heating and cooling are present in a building, internal heat recovery is present and only the net balance is handled through the network. Eq. (1) can be discretized using a time step $\Delta t$:

$$T_{in,i}(t+\Delta t) = exp\left(-\frac{\Delta t}{R_i C_i}\right) T_{in,i}(t) + \left[1 - exp\left(-\frac{\Delta t}{R_i C_i}\right)\right]\left[T_{am}(t) + R_i\left(\dot{Q}_{gain,i}(t) + \dot{Q}_{in,i}(t)\right)\right] \tag{2}$$

Values of thermal capacitance and thermal resistance vary from building to building. For estimating the values of $C$ and $R$, various methods can be applied based on measured historical data or detailed building simulation software. Here, we used to technique described in [33] to estimate these two values. First, EnergyPlus building archetype models from the U.S. Department of Energy (DOE) website [34] were adopted. The output results of the EnergyPlus models were used to fit the parameters in Eq. (2) for different buildings, assuming that their location was Quebec City (Canada). For households, the $R$ value that was obtained is 3.6 °C/kW and the $C$ value is 5.41 kWh/°C. Considering that there are differences between households and as [33] shows, a normal distribution can be used to describe the distribution of these parameters. Therefore, the $R$ and $C$ values for households were assumed to obey a normal distribution with the means mentioned above and standard deviations of 3.6 °C/kW and 0.552 kWh/°C. For the commercial building, the R value that was found with the same approach is 0.35 °C/kW and the C value is 25 kWh/°C. Note that the floor surface area of the house archetype was 221 $m^2$ and that of the commercial building archetype, 5000 $m^2$. Different numbers of buildings will be considered later in the application of the proposed methodology in order to consider small as well as large DHC systems.

The heat extracted from or rejected to the network by a building $i$ at time $t$ (thermal demand of the building from the network, $\dot{Q}_{net,i}(t)$) can be expressed as:

$$\begin{cases} \dot{Q}_{net,i}(t) = \dot{Q}_{in,i}(t)\dfrac{COP_H - 1}{COP_H} & if \quad \dot{Q}_{in,i}(t) > 0 \\ \dot{Q}_{net,i}(t) = \dot{Q}_{in,i}(t)\dfrac{COP_C + 1}{COP_C} & if \quad \dot{Q}_{in,i}(t) \le 0 \end{cases} \tag{3}$$

For buildings with thermostatically controlled loads, the electricity consumption is divided into the internal load (such as lights and electrical equipment) and the consumption of the heat pumps. The electricity consumption rate at time $t$ can be expressed as:

$$\begin{cases} \dot{E}_i(t) = \dot{Q}_{net,i}(t)\dfrac{1}{COP_H - 1} + \dot{E}_{in,i}(t) & if \quad \dot{Q}_{net,i} > 0 \\ \dot{E}_i(t) = -\dot{Q}_{net,i}(t)\dfrac{1}{COP_C + 1} + \dot{E}_{in,i}(t) & if \quad \dot{Q}_{net,i} \le 0 \end{cases} \tag{4}$$

In the present test case, the temperature set-point (without demand-side management) and occupancy profile (in person/m$^2$) in the residential and commercial buildings were adopted from the archetypes introduced above. The temperature set-point of the dwellings is 22 °C at all times. In the commercial building, the temperature setpoint during non-occupancy periods (from 0 h–6 h and after 22 h) is 15 °C and during occupancy is 22 °C. The maximal number of people is 268 for the commercial building and 5 in each house. The occupancy schedule (people/peak number of people) is shown in Fig. 2.

In the management system proposed here, the indoor temperature during occupancy time was allowed to vary from 20 to 24 for residences and commercial buildings. The temperature for non-occupancy time is allowed to vary from 15 to 30. Furthermore, the initial and final indoor temperatures were forced to be equal so that there is no variation of the energy stored in the buildings over the horizon considered (initial and final values of 22 °C and 15 °C were used for residential and commercial buildings, respectively). As will be explained in Section 2.5, an unsatisfaction function was calculated to characterize the extent to which the actual temperature departed from the set points.

### 2.3. Energy balance: data center

The electricity demand of the data center was separated into two parts. One portion is due to the consumption of the servers, and the other is devoted to the data center heat pump. We assumed that the electricity consumption rate from the servers, $\dot{D}_s(t)$, was entirely converted into heat. This heat must then be removed by the data center heat pump and eventually rejected into the thermal network. Therefore, one finds the total electricity consumption rate of the data center at a given time step:

$$\dot{E}_D(t) = \dot{D}_s(t) + \frac{\dot{D}_s(t)}{COP_C} \tag{5}$$

By energy conservation, the heat transfer rate exchanged with the network by the heat pump, $\dot{Q}_{net,D}$, is thus:

$$\dot{Q}_{net,D}(t) = \frac{-\dot{D}_s(t)}{COP_C}(1 + COP_C) \tag{6}$$

The negative sign means that the heat transfer rate is rejected into the network, based on the sign convention adopted above. Thus, the electricity consumption rate can be expressed as:

$$\dot{E}_D(t) = \dot{Q}_{net,D}(t) \tag{7}$$

Several demand response strategies for data centers have been proposed, studied, and tested in literature. As described in [35], data centers with "non-mission critical" assignments are particularly good candidates and can achieve high peak reductions. Examples of demand response strategies include adjusting temperature and humidity set-points, load shifting and management, and virtualization on the IT infrastructure side. Here, we considered the reduction of the power demand of the servers, which, in turn, would also reduce the cooling demand. In the present test case, the baseline is assumed to be a sine-like function of the time of the day with a peak demand at 12 h30 PM as proposed by Ref. [35]. More specifically, it was assumed that, if needed, the electric demand of the servers' data center could be reduced to 90% of its baseline demand $\dot{D}_s^*$, which translates mathematically as:

$$\begin{aligned} &90\%\dot{D}_s^*(t) \le \dot{D}_s(t) \le \dot{D}_s^*(t) \\ &\text{where} \quad \dot{D}_s^*(t) = \dot{D}_{base}^* + \dot{D}_A^* sin\left(\frac{t - 0.5}{24}\pi\right) \end{aligned} \tag{8}$$

In the end, Eqs. (6)–(8) describe the behavior of the data center and were integrated into the model in the form of constraints, as will be shown below.

### 2.4. Central plant system

As previously mentioned, it is necessary to balance out the energy demand of the whole network with central heating and cooling equipment since in general, the heat discharged by exothermic nodes will not be equal to the heat required by endothermic nodes. Introducing the net district requirement for heating and cooling $\dot{Q}_{net,Central}$ (a positive value means that heating is needed and a negative value means that cooling is required), it must be compensated either by the central electrical boiler or by the central chiller depending on whether heating or cooling is needed. This can be formulated as:

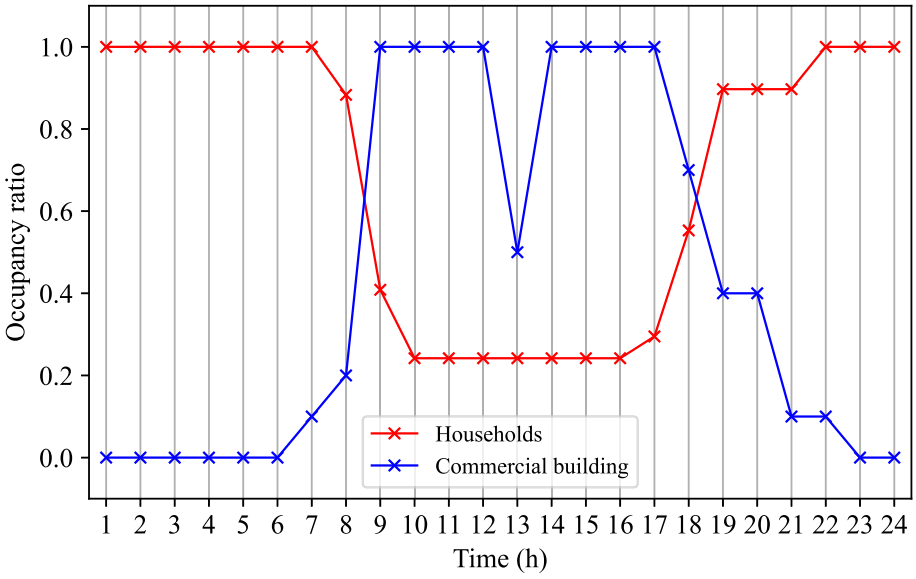


**Fig. 2.** Occupancy profile for commercial buildings and households in ratios [34].

$$\dot{Q}_{net,Central}(t) = -\dot{Q}_{Boiler}(t) + \dot{Q}_{Chiller}(t)$$

*s.t.*

$$\begin{aligned} &\dot{Q}_{Boiler}(t) \geq 0 \\ &\dot{Q}_{Boiler}(t)\dot{Q}_{Chiller}(t) = 0 \\ &\dot{Q}_{Chiller}(t) \geq 0 \end{aligned} \tag{9}$$

The term $\dot{Q}_{Boiler}(t)\dot{Q}_{Chiller}(t) = 0$ ensures that no simultaneous use of the boiler and chiller was possible. For simplicity, the capacity of the boiler and of the chiller was not limited, so that there is always enough thermal power to satisfy the demand of the whole district.

The electricity consumption of the central plant can easily be determined from:

$$\dot{E}_{Central}(t) = \frac{\dot{Q}_{Boiler}(t)}{\eta_{Boiler}} + \frac{\dot{Q}_{Chiller}(t)}{COP_{Chiller}} \tag{10}$$

One can perform a heat balance at the district level, resulting in a global constraint in the present model:

$$\dot{E}_{Central}(t) = \frac{\dot{Q}_{Boiler}(t)}{\eta_{Boiler}} + \frac{\dot{Q}_{Chiller}(t)}{COP_{Chiller}} \tag{11}$$

### 2.5. Unsatisfaction function

The unsatisfaction function is a subjective function that quantifyes the "unhappiness" of end-users when their heating or cooling demands are not fully satisfied.

For the data center, the unsatisfaction function was built by summing over each time step of the horizon considered (here 24 h) the square of the difference between the nominal demand $D^*$ and the actual demand $D$:

$$U_D = u_D \sum_{t=1}^{24} \left[\dot{D}_s^*(t) - \dot{D}_s(t)\right]^2 \tag{12}$$

where $u_D$ is a constant in $/kWh$^2$ for expressing the penalty in $. As can be seen from Eq. (12), the unsatisfaction function is a convex function related to the reduction of the demand which has been used in the past [36].

For buildings, we considered that the end users' discomfort is only related to the indoor temperature. This approach has often been used in the literature on buildings in which the loads are considered thermostatically controllable [37,38]. Therefore, for building $i$, the unsatisfaction function is defined as:

$$U_i = \sum_{\tau=1}^{24} u_i \omega_i(\tau)\left(T_{in,i}(\tau) - T_i^*\right)^2 \tag{13}$$

where $u_i$ is a constant in $\$/(person^*K^2)$ to express the discomfort of the building $i$ in $, $\omega_i$ is the occupancy profile (number of people) for building $i$ and $T_i^*(t)$ is 22 °C. In the present test case, the maximum number of people in each household was set to 5 and the occupancy profile is shown in Fig. 2. The maximum number of people in the commercial building is 268 people and the occupancy profile is also shown in Fig. 2.

The values of $u_D$ and $u_i$ are subjective values and depend on the willingness of the prosumers to adjust their demand. In this work, several combinations of these values were tested. In the end, the following values were used: $u_D = 5 \times 10^{-4}\left(\$/\text{MWh}^2\right)$ and $u_i = 5 \times 10^{-4}\left(\$/(\text{person} \bullet \text{K}^2)\right)$. These values appeared to offer a good tradeoff between flexibility and satisfaction for prosumers. It was verified that the selected value of $u_i$ did not lead to unrealistic indoor temperatures during optimization. That is why no indoor temperature bounds were explicitly enforced in the problem. We found that the cost of dissatisfaction with these u-values was <5% of the total cost in all cases tested, but this was enough to influence significantly optimal results. In future work, more values could be tested.

## 3. Energy management of 5GDHC based on centralized or distributed optimization

In this section, two energy management strategies of 5GDHC are formulated: one based on centralized optimization and one on distributed optimization. The centralized management of 5GDHC is first introduced in Section 3.1. A central coordinator who has the authorization to control all the pieces of equipment is responsible for making the optimal decision regarding their scheduling. Secondly, the distributed energy management of 5GDCH based on distributed optimization is introduced (Section 3.2). For each 5GDHC energy management strategy, we introduce below the objective function, constraints, and algorithms. Details and comparison of these two management strategies are then presented.

### 3.1. Energy management of 5GDHC based on centralized optimization and linearization of non-linear terms

The objective function of the centralized optimization can be formulated as follows:

$$\begin{aligned} J = &\underbrace{\Delta t\left\{\sum_{t=1}^{24} p_E(t)\left[\dot{E}_{Central}(t) + \sum_{i=1}^{N}\dot{E}_i(t) + \dot{E}_D(t)\right]\right\}}_{Part1} \\ &+ \underbrace{c_E\left\{max\left[\dot{E}_{Central}(t)\right] + \sum_{i=1}^{N} max\left[\dot{E}_i(t)\right] + max\left[\dot{E}_D(t)\right]\right\}}_{Part2} \\ &+ \underbrace{\left(U_D + \sum_{i=1}^{N} U_i\right)}_{Part3} \end{aligned} \tag{14}$$

where $p_E$ is the real-time electricity price ($/kWh) and $c_E$ is the electricity price for the peak power ($/kW). The objective function to minimize is the total operational "fee" $J$ of the whole district over 24 h. It consists of three parts: the first (Part 1 in Eq. (14)) is related to the cost of the electricity consumption of the whole district. It includes the electricity consumption of the central boiler, as well as that of the buildings (building-coupled heat pumps and electrical appliances) and of the data center. Part 2 accounts for the price of the electricity peak. Part 3 of the objective function is related to the discomfort of the end users, attributing a cost or a penalty to the unsatisfaction functions introduced in Section 2. Note that $N$ is the number of buildings.

This article aims at solving the optimization model with mixed integer quadratic programming. Therefore, each part of the objective function should be linear or quadratic, and the constraints should be linear.

Part 1 of the objective function is linear with respect to the electricity demands $\dot{E}_{Central}$, $\dot{E}_i$ and $\dot{E}_D$. $\dot{E}_D$ is linear with respect to the heat extracted from the network at the data center $\dot{Q}_{net,D}$. However, for nodes corresponding to buildings, $\dot{E}_i$ is not linear with $\dot{Q}_{net,i}$ as Eq. (4) shows. To linearize it, an auxiliary binary variable $\alpha$ and two continuous non-negative variables ($\dot{Q}_h$ and $\dot{Q}_c$) were introduced. When $\alpha = 1$, the heat pump extracts heat from the thermal network, and inversely, $\alpha = 0$ implies that the heat pump rejects heat to the thermal network. Therefore, $\dot{E}_i$ can be expressed as a linear relationship of $\dot{Q}_h$ and $\dot{Q}_c$. As a result, the net heat exchange with the network $Q_{net,i}$, the electricity consumed by a building $i$ ($E_i$) and the net heat received (or evacuated) at the building $Q_{in,i}$ are:

$$\begin{cases} \dot{Q}_{in,i}(t) = \dot{Q}_{h,i}(t) - \dot{Q}_{c,i}(t) \\ \dot{E}_i(t) = \dot{Q}_{h,i}(t)\dfrac{1}{COP_H} + \dot{Q}_{c,i}(t)\dfrac{1}{COP_C} + \dot{E}_{in,i}(t) \\ \dot{Q}_{net,i}(t) = \dot{Q}_{h,i}(t)\dfrac{COP_H - 1}{COP_H} - \dot{Q}_{c,i}(t)\dfrac{COP_C + 1}{COP_C} \end{cases}$$

$$\begin{aligned} s.t. \quad & \dot{Q}_{h,i}(t) \geq 0 \\ & \dot{Q}_{h,i}(t) \leq \alpha_i M \\ & \dot{Q}_{h,i}(t) \leq \dot{Q}_{h,max} \\ & \dot{Q}_{c,i}(t) \geq 0 \\ & \dot{Q}_{c,i}(t) \leq (1-\alpha_i) M \\ & \dot{Q}_{c,i}(t) \leq \dot{Q}_{c,max} \end{aligned} \tag{15}$$

where $M$ is a sufficient large number. That way, Part 1 of the objective function is now a linear expression of $\alpha, \dot{Q}_h$ and $\dot{Q}_c$.

For the central plant node, a constraint in Eq. (9) is non-linear due to the product $\dot{Q}_{Boiler}(t)\dot{Q}_{Chiller}(t)$. This can be reformulated as:

$$\begin{aligned} & \dot{Q}_{net,Central}(t) = -\dot{Q}_{Boiler}(t) + \dot{Q}_{Chiller}(t) \\ & s.t. \\ & \quad \dot{Q}_{Boiler}(t) \geq 0 \\ & \quad \dot{Q}_{Boiler}(t) \leq \alpha_{boiler} M \\ & \quad \dot{Q}_{Chiller}(t) \geq 0 \\ & \quad \dot{Q}_{Chiller}(t) \leq (1-\alpha_{boiler}) M \end{aligned} \tag{16}$$

where the big-M method introduced above was also used here to ensure that no simultaneous use of the boiler and of the chiller was possible. As a result, Part 1 of the objective function becomes linear with respect to $\dot{Q}_{Boiler}, \dot{Q}_{Chiller}(t)$ and $\alpha_{boiler}$.

Part 2 of the objective function is non-linear due to the max function. Therefore, auxiliary variables $z_i$ are introduced and the auxiliary constraints are added for the sake of linearization:

$$\begin{cases} z_{Central} \geq \dot{E}_{Central}(t) \quad \forall t \\ z_i \geq \dot{E}_i(t) \quad \forall t \\ z_D \geq \dot{E}_D(t) \quad \forall t \end{cases} \tag{17}$$

Part 3 is the unsatisfaction function that is a quadratic function of $\dot{D}_s$ (data center) and of the indoor temperature $T_{in}$. The indoor temperature $T_{in}$ is not linear with $\dot{Q}_{net,i}$, but is linear with respect to $\alpha, \dot{Q}_h$ and $\dot{Q}_c$:

$$\begin{aligned} T_{in,i}(t+\Delta t) = & \, exp\left(-\frac{\Delta t}{R_i C_i}\right) T_{in,i}(t) \\ & + \left[1 - exp\left(-\frac{\Delta t}{R_i C_i}\right)\right]\left[T_{am}(t) + R_i\left(\dot{Q}_{gain,i}(t) + \dot{Q}_{h,i}(t) - \dot{Q}_{c,i}(t)\right)\right] \end{aligned}$$

$$\begin{aligned} s.t. \quad & \dot{Q}_{h,i}(t) \geq 0 \\ & \dot{Q}_{h,i}(t) \leq \alpha_i M \\ & \dot{Q}_{h,i}(t) \leq \dot{Q}_{h,max} \\ & \dot{Q}_{c,i}(t) \geq 0 \\ & \dot{Q}_{c,i}(t) \leq (1-\alpha_i) M \\ & \dot{Q}_{c,i}(t) \leq \dot{Q}_{c,max} \end{aligned} \tag{18}$$

In the end, the decision variables chosen by the central coordinator are the thermal demands of all the buildings ($\alpha_i, \dot{Q}_{h,i}$ and $\dot{Q}_{c,i}$), the demand of the servers of the data center ($\dot{D}_s$) and the thermal output of the central plant ($\dot{Q}_{Boiler}, \dot{Q}_{Chiller}$ and $\alpha_{boiler}$) at each time step. The whole centralized 5GDHC energy management problem can be formulated as a mixed integer quadratic programming (MIQP) problem.

The constraints of the optimization problem are Eqs. (6), (7), (8), (10), (12), (13), (15), (16), (17), (18), as well as the global heat balance of the network, Eq. (11), which can be expressed as a function of the decision variables:

$$\frac{-\dot{D}_s(t)}{COP_C}(1 + COP_C) + \left[\dot{Q}_{Chiller}(t) - \dot{Q}_{Boiler}(t)\right] + \sum_{i=1}^{N}\left[\dot{Q}_{h,i}(t) - \dot{Q}_{c,i}(t)\right] = 0 \quad \forall t \tag{19}$$

Although the objective function to minimize ($J$) in this work only accounts for costs and dissatisfaction, future work could include other important objectives, such as minimizing greenhouse gas emissions and exergy destruction.

It is interesting to note that in the present problem, the so-called demand overlap coefficient (DOC) [39], a metric that can be used to characterize the synchronicity of the heating and cooling demands, is not known a priori because the heating and cooling demands of the prosumers constantly adjust to the cost, which depends on everyone's consumption. Instead, the proposed approach and market mechanism can be seen as a way to increase the DOC of the network. This idea is also valid with the problem formulation of Section 3.2.

### 3.2. Energy management of 5GDHC based on distributed optimization

As previously mentioned, centralized management is straightforward to formulate but can be hard to solve due to the scale of the problem, and it can also result in privacy issues. To deal with these problems, the Proximal Jacobian ADMM (alternating direction method of multipliers), which is a distributed multi-block parallel optimization, is considered. Essentially, PJ-ADMM solves iteratively such optimization problems by temporarily relaxing global constraints (i.e., constraints containing variables from multiple nodes) and by decomposing the centralized optimization problem into a set of sub-problems that can be solved with their own local constraints. The minimally required information from the resulting solutions is then used to verify the respect of the global constraints (in our case, Eq. (19)) and adapt the cost structure for the next iteration until convergence is achieved.

The first step is to decompose the centralized optimization. We first decomposed the objective function of the centralized optimization problem into N + 2 nodes (N buildings + data center + central plant):

$$\begin{aligned} & min \quad J = \sum_{i=1}^{N+2} J_i(\mathbf{Q}_{net,i}) \\ & J_i = \begin{cases} \Delta t \sum_{t=1}^{24} p_E(t)\dot{E}_i(t) + c_E z_i + U_i \quad i: Builidng \quad node \\ \Delta t \sum_{t=1}^{24} p_E(t)\dot{E}_{Central}(t) + c_E z_B \quad Central \quad plant \quad node \\ \Delta t \sum_{t=1}^{24} p_E(t) E_D(t) + c_E z_D + U_D \quad Data-center \quad node \end{cases} \end{aligned} \tag{20}$$

The optimization problem can then be formulated as a series of "smaller" optimization problems. For the building nodes, we have:

$$\begin{aligned} &min \quad J_i \\ &s.t. \\ &\quad Eqs.(13),(15),(19) \\ &\quad z_i \geq \dot{E}_i(t) \\ &Varing \quad \alpha_i, \dot{Q}_{h,i}, \dot{Q}_{c,i} \end{aligned} \tag{21}$$

Similarly, for the data center node, one can solve the following problem:

$$\begin{aligned} &min \quad J_D \\ &s.t. \\ &\quad Eqs.(6),(7),(8),(12) \\ &\quad z_D \geq \dot{E}_D(t) \\ &Varing \quad \dot{Q}_{net,D} \end{aligned} \tag{22}$$

And finally, for the central plant problem, the problem becomes:

$$\begin{aligned} &min \quad J_{Central} \\ &s.t. \\ &\quad Eqs.(10),(16) \\ &\quad z_{Central} \geq \dot{E}_{Central}(t) \\ &Varing \quad \alpha_{Boiler}, \dot{Q}_{Boiler}, \dot{Q}_{Chiller} \end{aligned} \tag{23}$$

As mentioned above, global constraints (i.e., Eq. (19)) are temporarily relaxed because these constraints include variables from multiple nodes. Eq. (19) corresponds to the network thermal balance at all the time steps, meaning that there are, in fact, 24 global constraints. Constraints that only contain the variables related to one node are defined as local constraints while constraints that are related to variables from different nodes are called global constraints.

At each iteration, the nodes communicate with the coordinator, and the procedure of the Proximal Jacobian alternating direction method of multipliers (PJ-ADMM) is as follows (a graphical representation of this pseudocode is provided in Fig. 3):

**Step 1: Initialization:**

All the decision variables are randomly initialized while respecting their local constraints. The vector $\boldsymbol{\lambda}$ (dual variables of the global constraints) is initialized to 0. Then, an iterative process is implemented.

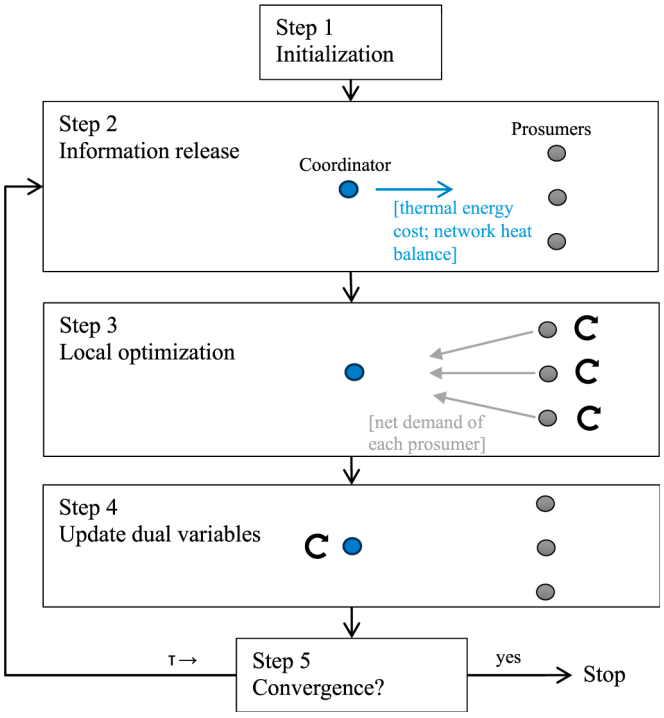


**Fig. 3.** Schematic representation of the distributed optimization approach.

**Step 2: Information release:**

The coordinator sends to the nodes the values of $\boldsymbol{\lambda}$ at the present iteration, as well as values of the sum of the thermal demand (the net heat extracted or rejected to the network) at each time step. At this point, the sum of the thermal demands might not be zero because, as mentioned above, the global constraint has been temporarily relaxed at this step.

**Step 3: Local optimization and submission of the updated thermal requirement:**

Each node optimizes its decision variables $\mathbf{x}$ based on the information transmitted by the coordinator according to the following equation:

$$\mathbf{x}_i^{k+1} = \underset{\mathbf{x}_i}{\operatorname{argmin}} \left[ \begin{aligned} &J(\mathbf{x}_i) + \boldsymbol{\lambda}^k \underbrace{\left[ \dot{\mathbf{Q}}_{net,i}(\mathbf{x}_i) + \sum_{j \neq i} \dot{\mathbf{Q}}_{net,j}^k \right]}_{Term1} \\ &+ \frac{\rho}{2} \underbrace{\left\| \dot{\mathbf{Q}}_{net,i}(\mathbf{x}_i) + \sum_{j \neq i} \dot{\mathbf{Q}}_{net,j}^k \right\|_2^2}_{Term2} \\ &+ \frac{\beta}{2} \underbrace{\left\| \dot{\mathbf{Q}}_{net,i}(\mathbf{x}_i) - \dot{\mathbf{Q}}_{net,i}^k \right\|_2^2}_{Term3} \end{aligned} \right] \tag{24}$$

$$s.t.$$

$$Local \quad constrains$$

where k is the iteration index. $\mathbf{Q}_{net,i} = \left[ Q_{net,i}(t=1), \ldots Q_{net,i}(t=24) \right]$ means the vector of the thermal energy exchange between the node $i$ and the network for the 24 h. If the node extracts heat from the network, $Q_{net,i}$ is positive, otherwise, $Q_{net,i}$ is negative. As can be seen in Eq. (24), instead of directly minimizing the cost J for each node, three additional terms are added into the objective function. The ADMM ensures that the solutions tend to satisfy the global constraints that are temporally relaxed when decomposing the centralized problem by adding penalty terms (term 1 and term 2). Indeed, when the global constraints are respected (i.e., convergence is achieved), terms 1 and 2 vanish. PJ-ADMM adds the term 3 to accelerate the convergence of the algorithm. Term 3 is a penalty term to avoid large changes between the iterations. Note that $\beta$ are $\rho$ are numerical coefficients that are adjusted depending on the problem to facilitate convergence [19].

Each node makes its decisions in parallel. Once the new decisions of each node have been made, the new thermal requirements of each time step ($\dot{\mathbf{Q}}_{net,i}$) to the network can be calculated. Each node will submit its new thermal requirements to the coordinator.

**Step 4: Gather information and update the dual variables:**

The coordinator receives the updated demands and updates the dual variable vector with:

$$\boldsymbol{\lambda}^{k+1} = \boldsymbol{\lambda}^k + \gamma\rho \sum_{i=1}^{N+2} \mathbf{Q}_{net,i}^{k+1} \tag{25}$$

where $\gamma$ is a damping parameter for updating the dual variable $\boldsymbol{\lambda}$. When the global constraints are respected, the right-hand side term becomes zero and the dual vector stops to change.

**Step 5: Check termination:**

The process is repeated until the global constraints are respected (i.e., Eq. (19)). That means the sum of the heat exchange between the prosumers (including the central plant) and the network is zero at each time step. Therefore, the termination criterion can be expressed as:

$$max\left|\sum_{i=1}^{N+2}\mathbf{Q}_{net,i}^{k+1}\right| < \varepsilon \quad or \quad k > k_{\max} \tag{26}$$

If these conditions are not respected, the iteration index k is incremented, and we go back to step 2.

As mentioned above, for the PJ-ADMM algorithm, the coefficients $\beta$, $\rho$ and $\gamma$ are hyperparameters. It can be proved that if the three parameters satisfy the following constraints, the algorithms can converge within a limited number of iterations [19]:

$$\begin{aligned}&\frac{\beta}{2} > \rho\left(\frac{N+2}{2-\gamma} - 1\right)\\ &0 < \gamma < 2\end{aligned} \tag{27}$$

Eq. (27) provides a guideline for choosing $\beta$,$\rho$ and $\gamma$. In our case, the hyperparameters were tuned by trial and error.

The update process of PJ-ADMM can easily be parallelized since the optimization problem of each node can be solved separately at each iteration. From step 3, the only information that the node i received is the sum of the thermal demand of the others. As a result, the prosumer is blind to other prosumers' personal information, such as occupancy profiles and cannot directly control the other prosumers' appliances. The coordinator only knows the thermal demand of the prosumers.

### 3.3. Community-based transactive market

Based on the algorithm of PJ-ADMM, we proposed a market clearing procedure. We define our payment rule at each time step as the product of the dual variable and the heat exchange between the prosumer and the network:

$$\pi_i(t) = \lambda(t) Q_{net,i}(t) \tag{28}$$

where $\pi_i(t)$ is the amount (in $) received or paid by node $i$ at the time t. $\pi_i(t)$ can be positive or negative, meaning respectively that the prosumer i will either have to pay or will receive money for its participation to the network at that particular instant. Positive $\pi_i(t)$ are achieved when $\lambda$ and $Q_{net,i}$ have the same sign. For example, this occurs when i needs heat from the network (positive $Q_{net,i}$) and the network globally has a deficit of heat ($\lambda$ positive). Inversely, if node i needs reject heat ($Q_{net,i} < 0$) and $\lambda > 0$, node i will be retributed (negative $\lambda$ means there exists sufficient heat source in the district).

The payment rule proposed in this article thus has a "uniform price" market structure [23], which means that at a given time step, the internal thermal energy price is the same for all nodes.

Eq. (24) can be reformulated as:

$$\mathbf{x}_i^{k+1} = \underset{\mathbf{x}_i}{\operatorname{argmin}} \left[ \begin{array}{l} \underbrace{J(\mathbf{x}_i) + \boldsymbol{\lambda}^k \dot{\mathbf{Q}}_{net,i}(\mathbf{x}_i)}_{Term1} \\ \underbrace{+\frac{\rho}{2}\left\| \dot{\mathbf{Q}}_{net,i}(\mathbf{x}_i) + \sum_{j\neq i} \dot{\mathbf{Q}}_{net,j}^k \right\|_2^2}_{Term2} \\ \underbrace{+\frac{\beta}{2}\left\| \dot{\mathbf{Q}}_{net,i}(\mathbf{x}_i) - \dot{\mathbf{Q}}_{net,i}^k \right\|_2^2}_{Term3} \underbrace{+\boldsymbol{\lambda}^k \sum_{j\neq i} \dot{\mathbf{Q}}_{net,j}^k}_{Term4} \end{array} \right] \tag{29}$$

*s.t.*

*Local constrains*

This reformulation highlights the objective function of node $i$ without the penalties (Term 1). Term 1 is the sum of the electricity bill, unsatisfaction function and payment of node $i$ for its usage of the network. Term 2 is the penalty of the global constraints, and term 3 can be seen as the penalty for adjusting the thermal demand from the last iteration. Finally, term 4 is not related to the decision variables, so it does not influence the optimal solution. As can be seen, the iterative optimization procedure introduced in the previous section corresponds to a market clearing process in which each prosumer submits their initial thermal requirement to the coordinator. Then, the network coordinator communicates the internal thermal prices $\boldsymbol{\lambda}$ to each prosumer. Prosumers continue to adjust their thermal demand with Eq. (29) while the coordinator continues to adjust the price until the global constraint (energy balance) is respected.

## 4. Analysis of the properties of the proposed market mechanism

By defining the payment rules, we have established a market mechanism for the energy interaction between the prosumers of a 5GDHC network. As mentioned in the literature review presented in Section 1, when doing so, it is advisable to examine the properties of that mechanism. Four desirable properties are commonly used for analyzing a market mechanism and were presented in the introduction. Before talking about the properties, it is worth mentioning that we assumed here that all the prosumers of the 5GDHC were honest and gave real information to the centralized or distributed optimizers. In other words, no market player desires to exercise "market power" by behaving "strategically". The impact of such fraudulent behaviors is outside the scope of the present study and could be the object of future work. Under the assumption of perfect competition, the four properties of our market mechanism are discussed below.

**Property 1: Efficiency**

The terms 2 and 3 of Eq. (24) will be nearly zero when the optimization is near convergence. This means that the solution is optimal for each prosumer under the designed payment. In other words, no prosumer has advantage to deviate unilaterally from its dispatch. As mentioned in the literature review, there exists a duality gap between the solution of centralized and distributed optimizations for functions that are not convex. The optimization problem introduced above is a mixed integer quadradic programming, i.e., it is not convex. Therefore, a comparison between the optimal results of the centralized and distributed algorithms should be made. Section 5.1 shows that the duality gap is small in the cases tested.

**Property 2: Incentive compatibility**

The mechanism in this paper cannot guarantee that all the participants act truthfully. This is the main drawback of the "uniform price" mechanism. A simple example can be that if the central plant tells the optimizer that its unit cost for generating heat is $100/MWh while the truth is $84/MWh, the coordinator must accept this price when the other prosumers cannot be balanced. However, this would reduce the profit of the heating demand users, and the minimization of the cost of the whole district is not guaranteed.

**Property 3: Budget balance**

The payment rule of the coordinator is the term 2 of Eq. (29). Once the distributed optimization terminates, the total payment is:

$$\pi(t) = \sum_{i=1}^{N+2}\pi_i(t) = \sum_{i=1}^{N+2}\lambda(t)Q_{net,i}(t) = \lambda(t)\underbrace{\sum_{i=1}^{N+2}Q_{net,i}(t)}_{0} = 0 \tag{30}$$

Eq. (30) ensures the overall budget balance.

**Property 4: Individual rationality**

If the network cannot balance itself, boilers or chillers in the central plant will be used. It can be proven that the real-time internal energy price will never be higher than the real-time unit cost of the central plant system for constant and Time-Of-Use electricity price rates. The proof is available in Appendix A. However, this may not hold true for the Charge-For-Peak electricity rate. Appendix A proves that the peak electricity price will be allocated into different periods and under this

situation, the prosumer may loss benefit.

## 5. Results and analysis of proposed market mechanism based on case-study scenarios

The centralized and distributed energy management systems introduced above were tested for different virtual districts and different electricity tariffs. The weather of a typical winter day (Feb 21st, 2020) in Quebec City (Canada) was chosen (the weather file can be downloaded from [40]). Three common electricity price structures were considered and are summarized in Table 2: a constant electricity price (ConsP), a Time-Of-Use electricity price (TOU) and a charge for peak electricity price (C4P).

The simulation plan is detailed in Table 3. Section 5.1 compares the performance of the centralized and distribution optimization approaches. In that section, two districts were used to evaluate the gap between the algorithms and the calculation times: one small district (12 nodes) and one large (73 nodes). Section 5.2 studies how the internal thermal energy price, as well as the heat and cold demands are affected by the electricity tariffs, with the help of the 73-node district. In Section 5.3, the size of the data center within the 73-node district is varied to develop a better understanding of how the proposed framework adapts to different ratios between the heat and cold demands. Finally, Section 5.4 analyzes the motivation of the coordinator and prosumers by comparing their benefits to the situation in which no district heating and cooling network would exist. Without a thermal network, all the buildings are disconnected from the thermal network, and each prosumer has their own boilers with an efficiency of 95% and chillers with a COP of 3.5. The value of the unsatisfaction function for these reference scenarios is zero for all the prosumers.

All the optimization problems are solved on a Windows-based PC (8 cores I7 3.8GHz) with 32GB of RAM with the help of Matlab parallel box.

### 5.1. Comparison between centralized and distributed optimization

As mentioned above, we used two district sizes to compare the performance of the centralized and distributed optimization algorithms: a small-scale district (12-node case) consisting of 10 houses and one small data center ($\dot{D}^*_{base}$=7 kW, $\dot{D}^*_A$=14 kW), and a large-scale district (73 nodes) consisting of 70 houses, one commercial building and one data center ($\dot{D}^*_{base}$=70 kW, $\dot{D}^*_A$=140 kW). The three cost structures for electricity were considered for each type of optimization and for each district.

For the distributed optimization algorithm, a stop criterion is necessary (see Eq. (26)). Here, the stop criterion was that the maximum of the unbalanced power is smaller than 100 W, which is relatively small compared with the thermal demand of any node of the district (from 3 kW to 300 kW). To illustrate the convergence of the distributed optimization algorithm, Fig. 4 shows an example of the residual of the heat balance for the large-scale district with the distributed optimization and with the charge for peak tariff. Similar curves were observed for the other network and cost structures. For the three price structures, the distributed optimization converges within 552 iterations or less for this district (73 nodes), the charge for peak price being the cost structure requiring the most iterations to converge.

The convergence of the distributed optimization means that the algorithm succeeded in finding a solution. However, as mentioned before, there is a duality gap between the solution of the centralized and distributed optimizations. The objective function calculated with PJ-ADMM and those obtained with the centralized optimization approach were thus compared. Table 4 shows that the duality gap, which can be seen as the difference between the solutions of the centralized and decentralized solvers, is smaller than 5% for the different districts and electricity tariffs tested in the present work. This means that the decentralized solver can successfully find solutions close to those that the omnipotent centralized solver identified. The computational time for the distributed optimization is about 20% shorter than that of the centralized optimization for the larger district. However, the advantage of distributed optimization for time-saving is not present for smaller districts. With only 12 nodes (small district), the centralized optimization requires ~10 s of computational time, while the distributed optimization takes ~40 s. Therefore, the benefits of distributed optimization in terms of computational time only become apparent as the number of prosumers increases.

**Table 2**
The three electricity tariffs studied in this work.

| Constant (ConsP) | Time-of-use (TOU) | Charge for peak (C4P) |
|---|---|---|
| • $0.08/kWh | • 8 PM-4 AM: $0.05/kWh<br>• Noon-5 PM: $0.113/kWh<br>• Else: $0.17/kWh | $0.06/kWh + $0.4/kW (daily peak) |

**Table 3**
Simulation plan performed in this work with various energy management approaches, electricity tariffs and districts.

| Section | Energy management approach | Electricity tariffs | Case-study districts |
|---|---|---|---|
| Section 5.1 | • Centralized<br>• Decentralized | • Const<br>• TOU<br>• C4P | • Small district −10 houses -Small data center ($\dot{D}^*_{base}$=7 kW, $\dot{D}^*_A$=14 kW)<br>• Large district −70 houses +1 commercial building -Med. data center ($\dot{D}^*_{base}$=70 kW, $\dot{D}^*_A$=140 kW) |
| Section 5.2 | • Distributed | • Const<br>• TOU<br>• C4P | • Large district (as above) |
| Section 5.3 | • Distributed | • TOU | • Large district with variable data center sizes: -Small ($\dot{D}^*_{base}$=60 kW, $\dot{D}^*_A$=120 kW) -Med. ($\dot{D}^*_{base}$=70 kW, $\dot{D}^*_A$=140 kW) -Large ($\dot{D}^*_{base}$=120 kW, $\dot{D}^*_A$=240 kW) |
| Section 5.4 | • Distributed<br>• No district | • Const<br>• TOU<br>• C4P | • Large district with variable data center sizes |

### 5.2. Dynamic behavior of internal price and thermal demands as a function of electricity tariffs

This section aims to better understand the dynamic behavior of thermal energy price and demand with the proposed distributed framework. This was illustrated with the large-scale district and the three electricity price structures that had been introduced previously.

Fig. 5 reports the internal price for thermal energy (i.e., λ) and the thermal demand with a constant electricity price, as optimized by the proposed framework. In Fig. 5a, the price of the heat produced by the central boiler and that of the cold from the central chiller are constant over time due to the electricity cost structure. Note that a positive internal price means that a prosumer needs to pay for extracting heat from the network, and inversely, a negative internal price means that one needs to pay for rejecting heat into the network.

Appendix A proves that with the constant and TOU price structures, the boiler is only turned on when the instantaneous internal thermal

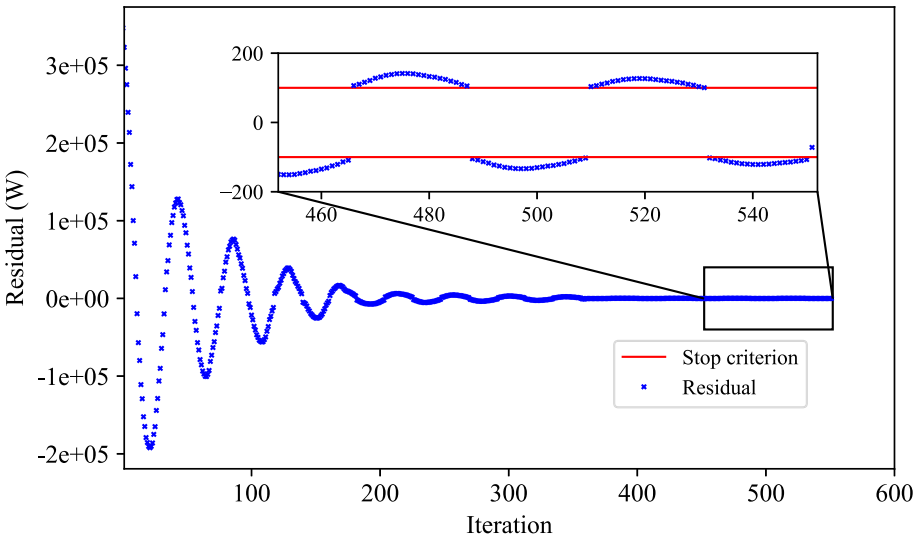


**Fig. 4.** Residual of the thermal balance (unbalanced power) as a function of the number of iterations for a large-scale district (73 nodes) with a charge for peak electricity price with the distributed optimization approach.

**Table 4**
Comparison of the minimized objective function and computational time achieved by the distributed and centralized optimization for small- and large-scale districts.

| Cases | | Optimization method | Total objective | Computational time (s) | Duality gap |
|---|---|---|---|---|---|
| Small-scale district (12 nodes) | ConsP | Centralized | $99.17 | 9 | |
| | | Distributed | $99.47 | 34 | 0.3% |
| | TOU | Centralized | $126.65 | 8 | |
| | | Distributed | $128.69 | 32 | 1.5% |
| | C4P | Centralized | $96.29 | 10 | |
| | | Distributed | $99.83 | 45 | 3.6% |
| Large-scale district (73 nodes) | ConsP | Centralized | $864.42 | 4231 | |
| | | Distributed | $871.26 | 3460 | 0.79% |
| | TOU | Centralized | $1099.83 | 4780 | |
| | | Distributed | $1116.15 | 3216 | 1.5% |
| | C4P | Centralized | $866.51 | 4300 | |
| | | Distributed | $900.55 | 3682 | 4% |

price is equal to the boiler's cost for heat production. Similarly, the chiller only operates when the internal price is equal to the chiller's own cost for producing cold. For example, in Fig. 5a, during the time steps 1 to 9 and 19 to 24, the boiler is on because the heating demand is much higher than the cooling demand and the network cannot be balanced without the central plant. When the internal price falls between the two unit costs (i.e., that of the boiler and chiller), it means that both the boiler and chiller are offline. In that case, the heat extracted from the network by the heat demand prosumers is equal to the heat rejected to the network by the cooling demand prosumers. In Fig. 5, this happens between time steps 10 to 18 inclusively. During these time steps, the demands are balanced. Heating demand prosumers can be considered as the "virtual chiller" of cooling demand prosumers. Similarly, the cooling demand prosumers can also be seen as the "victual boiler" of the heating demand prosumers.

In the beginning (hours 1 to 4 in Fig. 5), the heating thermal load is significantly reduced compared to the baseline (i.e., the actual heat demand in the absence of the present market mechanism). Because there is a low cooling demand from the data center during that period (i.e., the exothermic prosumers reject a small amount of heat), the internal thermal price has to be high because the boiler operates. Dissatisfaction of heat demand prosumers had to be created in order to reduce the cost. From hours 5 to 9, the baseline heating and cooling demands are satisfied, otherwise the building temperature would keep dropping and would not respect the minimal temperature threshold.

From 10 to 18 h, the internal price goes down because of the lower heating demand and higher cooling demand, allowing a demand balance with no boilers or chillers operating. Therefore, during that period, heating demand prosumers extract more heat than in the baseline situation, and the cooling demand prosumers reduce their cooling demand in order to reach a thermal balance.

After 18 h, the internal price goes up again because of the simultaneous low availability of waste heat (i.e., heat to be rejected by the cooling demand) and the increase of the heating demand. However, compared with the baseline, the heating demand of the prosumers is reduced at 19 h and 20 h. This is because the internal price is high, and prosumers prefer paying less and increase their dissatisfaction. The buildings cannot be further cooled down near the end of the day due to the constraints on the temperature and because the initial and final indoor temperatures were forced to be equal (see Section 2.2).

As can be expected, electricity price influences thermal demand because prosumers consume electricity while using their heat pumps to exchange heat with the thermal network. Fig. 6 shows the internal thermal price and the thermal demand of the district for the TOU electricity price structure. In contrast with the results under a constant electricity price, at the beginning of the day, prosumers increased their heating demand due to the low price of electricity and the internal price (1 h–4 h). The heat can be stored in the building and released later when the thermal energy price is higher. Both the heating and cooling demands are reduced when the electricity price is high at steps 5 and 6. At time steps 7 to 9, the internal thermal price is high. Therefore, the heating-dominated prosumers reduce their demand.

The internal price under Charge for Peak electricity rate is shown in Fig. 7. As Appendix A proves, the peak price is allocated into different periods. Differently from the two previous electricity price structures, the charge for peak electricity price puts a large penalty on the peak demand for each prosumer. Therefore, at the beginning of the day, buildings prefer reducing their heat demand and during time steps 14 to 17, they preheat their buildings to avoid the "increasing behavior" that happens in the constant and TOU price scenario (see the time steps 21 to 24 in Fig. 7).

In summary, it can be seen that with the proposed framework, the internal price for thermal energy and the demand of the prosumers dynamically adapt, trying to balance out the network and reduce costs, and that this transient behavior is strongly affected by the electricity cost structure.

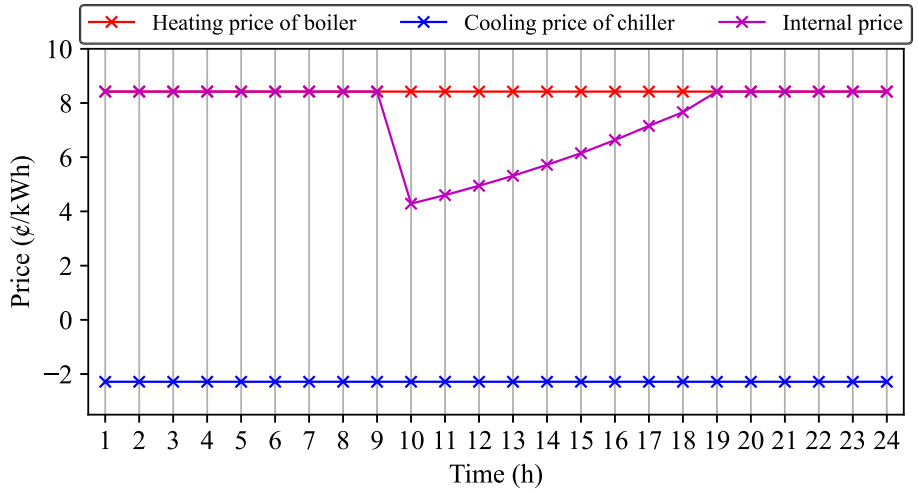


(a)

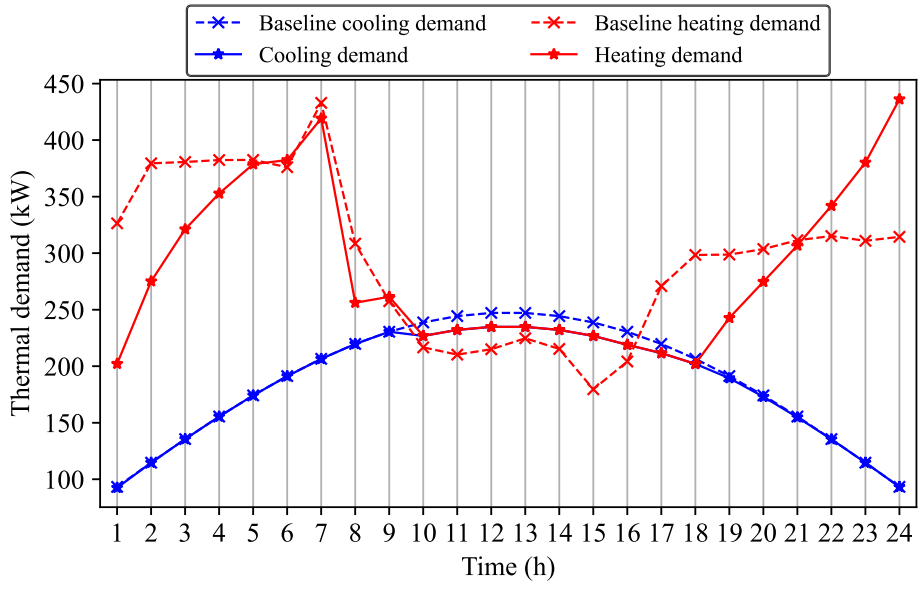


(b)

**Fig. 5.** (a) Internal price and (b) demand profiles with the medium size data center (Case M) and with constant electricity price.

### *5.3. Impact of heat availability on internal price, thermal demands, and cashflows*

In order to understand how the proportion of cold demand versus heat demand impacts the results of the proposed optimization framework, the size of the data center was varied (see Table 3). Three sizes were considered: small (S), medium (M) and large (L), respectively with $\dot{D}^*_{base}$=60, 70, 120 kW and $\dot{D}^*_A$=120, 140, 240 kW. For the sake of simplicity, only one electricity tariff was used in the present section (TOU).

Fig. 8 reports the internal price for the thermal energy and the thermal demands for the districts with the three data center sizes. A bigger data center means that there is more "free" heat available for heat-demand prosumers, which tends to reduce the internal price. When the internal price becomes negative, it means that the heat-demand prosumers will get paid to extract heat from the network, and inversely, cooling-demand prosumers will have to pay to reject heat into the network. This happens in the district with the large data center from 5 to 19 h. In fact, one can see in Fig. 8 that the central chiller operates from 8 to 16 h and that the system is balanced from 5 to 7 h and from 17 to 22 h. It can also be noted that the heat extracted from the network by the heat-demand prosumers is, in fact, higher than the baseline in most of this time interval. With the smaller data centers, the internal price always stays positive, meaning that the heat-demand prosumers will always need to pay to extract heat from the network, even though the internal price is always lower or equal to that of the boiler. In these cases, a heat balance is reached from 10 to 19 h (except at 16 and 17 h for the district with the smallest data center).

To better understand how heat and money are transferred within the network, flow diagrams were plotted. Figs. 9 and 10 show the heat flow and cash flow at the same time step ($t$ = 8 h) for different scenarios (small or large data centers).

With the small data center, the data center needs to reject 160 kW, which will demand 28.3 kW of electricity to drive the heat pump. Therefore, a total amount of heat of 188.3 kW is rejected into the network. The residential and commercial buildings need a total of

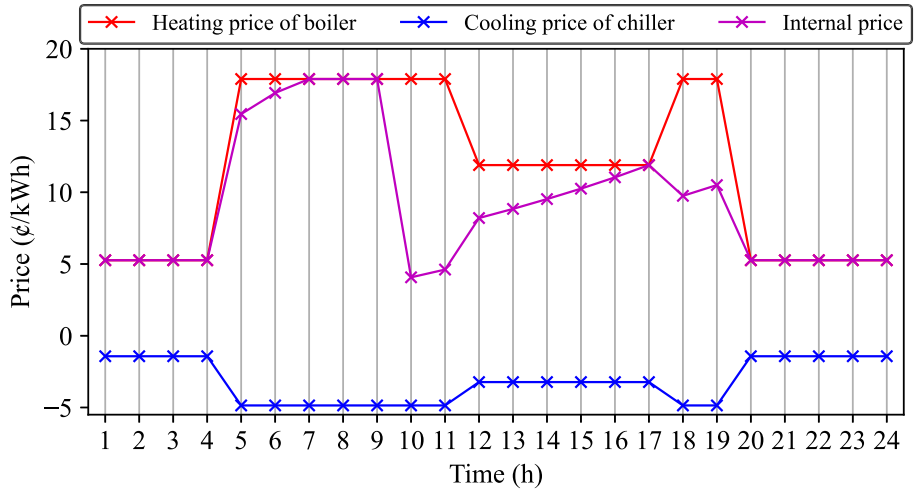


(a)

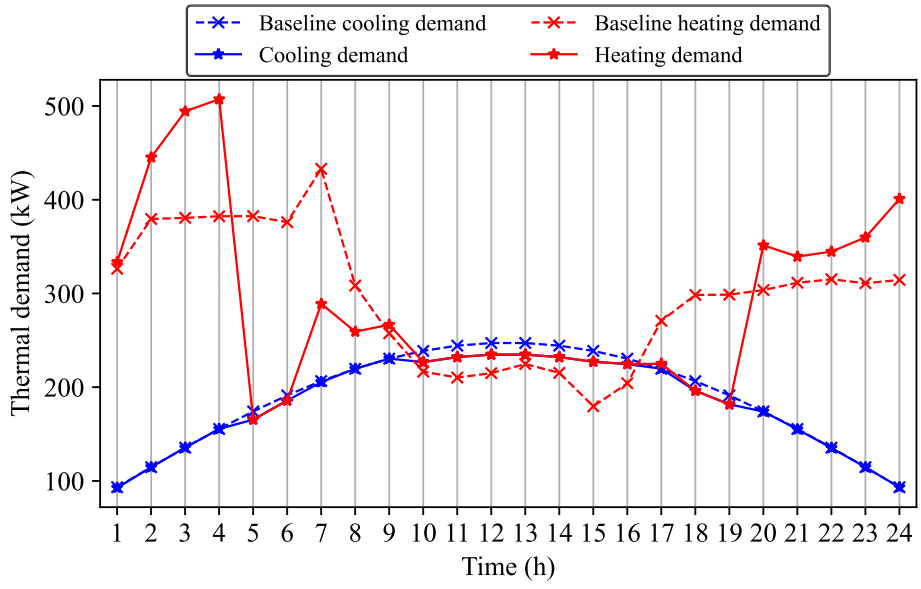


(b)

**Fig. 6.** (a) Internal price and (b) demand profiles with the medium size data center (Case M) and with time of use electricity price (TOU).

415.23 kW, i.e., 138.41 kW from the heat pump electricity consumption and 276.82 kW from the network. The available heat is insufficient, so that the boiler operates and outputs 88.52 kW of heat to balance the network. The internal price is 17.8¢/kWh. That means the data center and boiler will be paid for by the houses and commercial buildings, as Fig. 8 shows.

The situation is different for the large data center district (Fig. 10). In that case, the data center needs to reject 320 kW. Thus, the heat pump needs 56.6 kW of electricity to be powered. Therefore, 376.6 kW is rejected to the network. The house and commercial buildings need a total of 477.3 kWh: 159.1 kWh from the heat pump and 318.2 kWh from the network. The system is unbalanced and the chiller needs to operate and outputs 58.4 kWh of cooling to balance the network. The internal price is −5¢/kWh. That means the houses and commercial buildings, as well as the chiller, will get paid from the data center as Fig. 10 shows.

### 5.4. Benefits for coordinator and prosumers

This section explores the benefits of the proposed system and market mechanism compared to a situation in which no heating and cooling network would be present. In that case, all buildings would satisfy their own thermal demand with their own equipment. This analysis can help to understand the motivations of the coordinator and prosumers to participate in such a network. To compare the performance of the 5DGHC system with that achieved without it (hereafter called the "reference scenario"), the following indicators were used:

(i) Reduction of the total electricity consumption;
(ii) Reduction of the total peak electricity demand;
(iii) Reduction of the required capacity of the heating sources (boilers);
(iv) Reduction of the required capacity of the cooling sources (chillers).

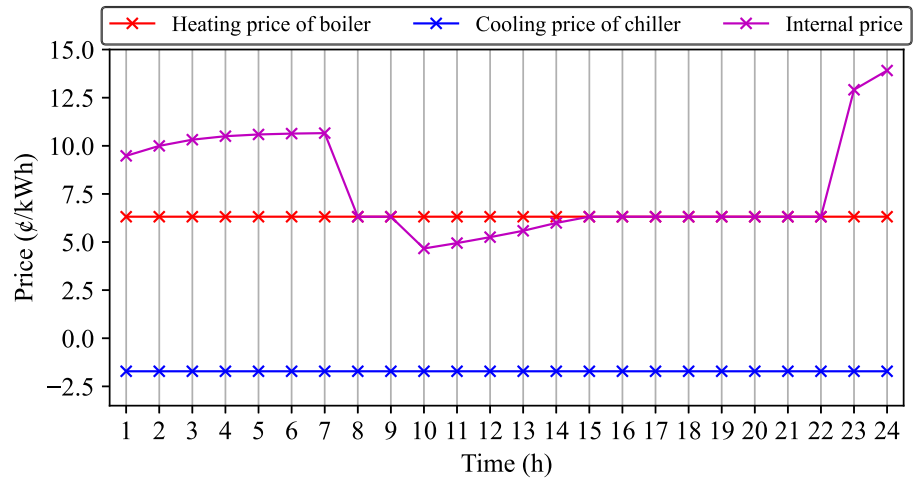


(a)

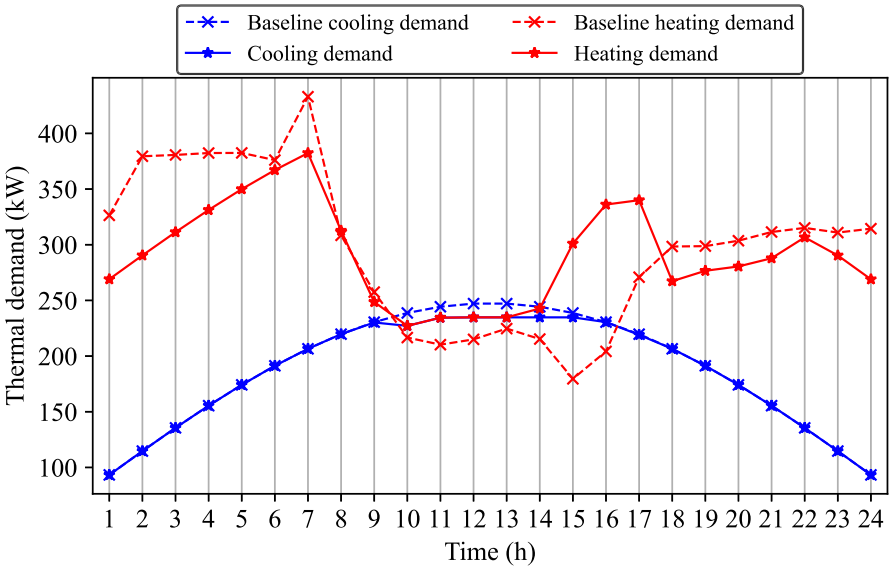


(b)

**Fig. 7.** (a) Internal price and (b) demand profiles with the medium size data center (Case M) and with charge-for peak electricity price (C4P).

These high-level indicators are collective indicators that can be related to the motivation of the coordinator, i.e., the central management of the system. These indicators were analyzed for the M districts from the previous section (i.e., the 73-node district with medium data center) and the three electricity tariffs.

Table 5 shows the results for the district with the medium data center under different electricity rates. Thanks to the "free heat" rejected from the data center, the total electricity consumption is reduced by 39–40% compared with the reference scenario with all tariffs. The C4P tariff exhibits the highest peak demand reduction because, for constant and TOU rates, the variation of the internal energy price may introduce some "pre-heating" and generate new peaks. It can also be seen in Table 5 that the chiller can be totally eliminated for this case because the waste heat rejected form the data center can be fully recovered. The capacity of the boiler is also reduced due to the available free heat. Finally, even though the network was not optimized to minimize exergy destruction, Table 5 reports that the 5GDHC reduces by 52–53% the rate of exergy destruction compared to the reference scenario without 5GDHC.

The motivation of the prosumers to participate to the 5GDHC system is to reduce the net cost that they have to pay. It should be remembered that the net cost means the sum of the electricity bills (positive), the payment (which can be positive or negative) for heat exchange with the network and the penalty for the discomfort or reduction of demand. Therefore, the reduction of the prosumers' operational cost was considered as the key performance indicator to quantify the benefit of the network from the prosumers' perspective. An example of electricity cost reduction for households (i.e., a sum of the 70 houses), commercial building and data center is reported in Table 6 for the three electricity tariffs.

Previous sections have shown that prosumers reduce (or at least do not increase) their operational cost under constant and TOU electricity rates, which is visible in the results of Table 6. Even though for the cases tested with the charge-for-peak tariff, all prosumers also gained benefits, it should be reminded that there is no guarantee of individual rationality in that case. In the cases reported in Table 6, the most important reduction was achieved for the data center since, in the district, the net demand is usually for heat. Thus, the data center is retributed by the payments of the other heat-demanding buildings.

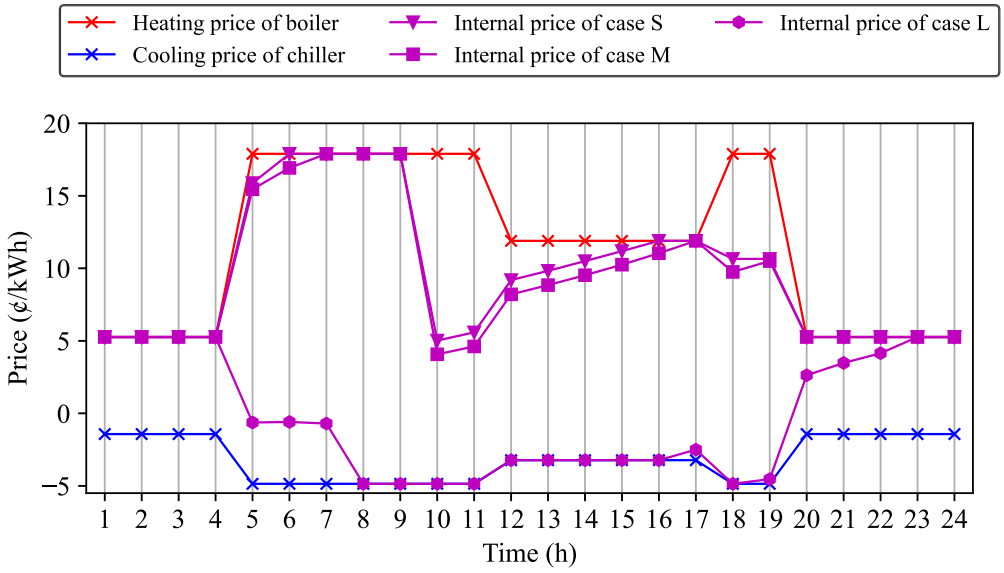


(a)

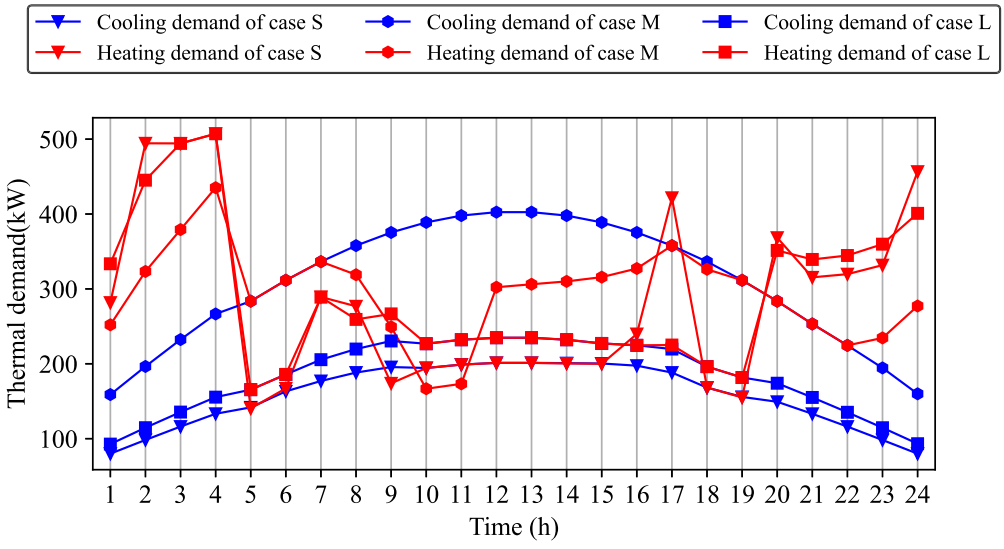


(b)

**Fig. 8.** (a) Internal price and (b) demand profiles pf different cases with TOU electricity price.

Finally, it is worth saying a few words about the discomfort costs, i.e., how much the prosumers are willing to sacrifice in terms of comfort/demand. The corresponding term in the objective functions affects not only the prosumer itself but also the whole district since it has an impact on the internal price of thermal energy. Table 7 reports a breakdown of costs and dissatisfaction for three variations of the district under the TOU tariff: (i) the situation without the 5GDHC system, (ii) a case with a loose dissatisfaction penalty corresponding to what was used in the present paper, and (iii) a case with a strong dissatisfaction penalty. The strong penalty was obtained by increasing the value of $u_D$ and $u_i$ introduced above to $5 \times 10^4 \left(\$/\text{MWh}^2\right)$ and $5 \times 10^4 (\$/(\text{person} \bullet \text{K}^2))$, respectively. In the absence of a district heating and cooling system (first column of result in Table 7), no dissatisfaction is created since every prosumer individually meets its own demand. When the 5GDHC system is introduced with a loose dissatisfaction penalty, the costs for the electricity used for heating/cooling are significantly reduced for all prosumers, including houses (from 970$ to 735$), the commercial building (from 270$ to 235$) and the data center (from 566$ to 74$). However, dissatisfaction is created to aim to balance the network. For houses and the commercial building, difference with the target temperature generated 10,209 and 6432 person·K$^2$ of discomfort, respectively. For the data center, a reduction of demand of 97.5 MWh was needed. With the strong penalty (last column of Table 7), prosumers are less willing to deviate from their baseline demand. That means the thermal demand is not sensitive to the internal price and for the coordinator, it becomes hard to balance the thermal requirement without using the boiler or the chiller. In fact, in the case presented in Table 7, no dissatisfaction was generated, meaning that the baseline demand of each prosumer could actually be met. Compared to the scenario with the loose penalty, the electricity costs of the houses and commercial building are only weakly affected by the stronger penalty. However, for the data center, the strong penalty increased the cost of electricity to 322$

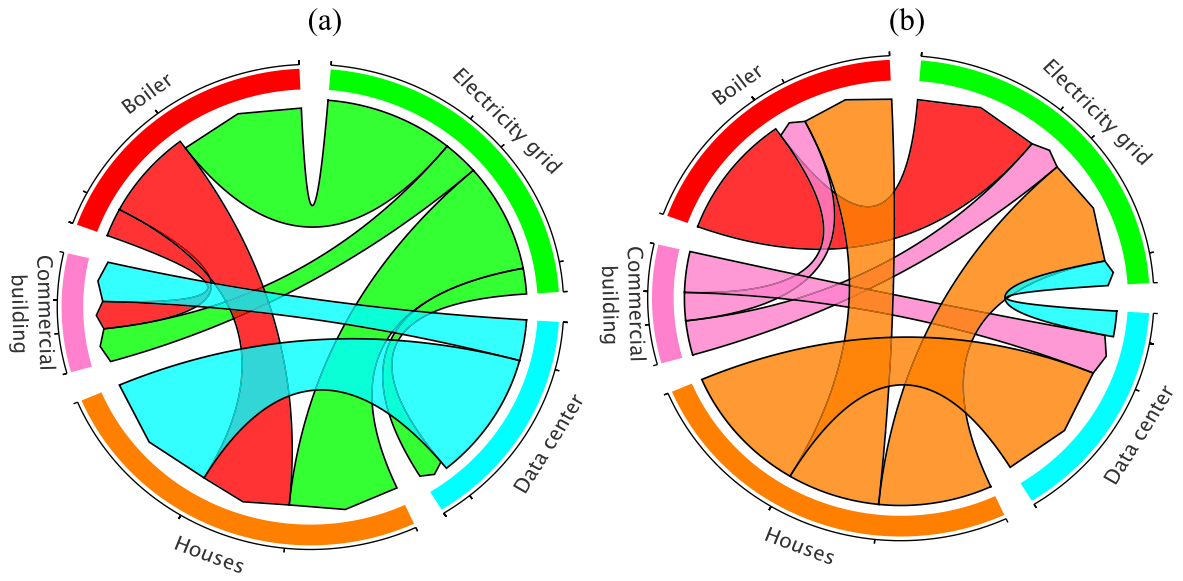


**Fig. 9.** (a) Heat flow and (b) cash flow in the 73-node district with the small data center with TOU tariffs at time step 8, colored by the origin of the flow.

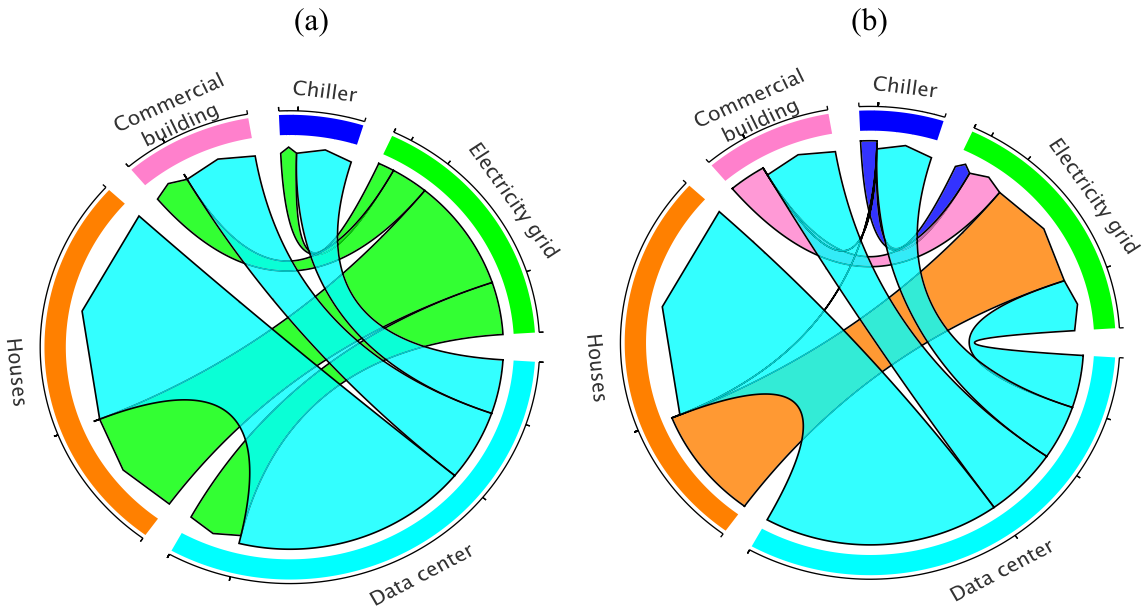


**Fig. 10.** (a) Heat flow and (b) cash flow in the 73-node district with the large data center with TOU tariffs at time step 8, colored by the origin of the flow.

**Table 5**
Comparison of global performance indicators with and without 5GDHC system, under different electricity tariffs for large district with medium data center.

| | Electricity tariff | | |
|---|---|---|---|
| | Constant | TOU | C4P |
| Reduction of electricity consumption (%) | 39.95 | 39.16 | 38.92 |
| Reduction of peak electricity demand (%) | 39.56 | 32.49 | 46.48 |
| Reduction of boilers capacity (%) | 50.00 | 47.69 | 74.37 |
| Reduction of chillers capacity (%) | 100 | 100 | 100 |
| Reduction of exergy destruction (%) | 53.88 | 52.54 | 52.35 |

**Table 6**
Comparison of cost reduction for prosumers with and without 5GDHC system, under different electricity tariffs for large district with medium data center.

| | Electricity tariff | | |
|---|---|---|---|
| | Constant | TOU | C4P |
| Reduction of cost for households (%) | 24.42 | 22.38 | 25.70 |
| Reduction of cost for commercial building (%) | 14.73 | 11.31 | 19.09 |
| Reduction of cost for data center (%) | 86.05 | 88.28 | 88.21 |

compared to 74$ with the loose penalty. The reason behind is that from 10 h00-15 h00, the strong penalty on discomfort forces the heating customer not to increase their demand so that the net demand of the district is cooling and therefore, the cooling price is the chiller's price that is more expensive compared with loose penalty scenario during 10 h00-15 h00 (see Fig. 7). It should be reminded that the discomfort penalty (i.e., the value of $u_D$ and $u_i$) is a somewhat subjective parameter and in practice, it would depend on the prosumer.

## 6. Conclusion and future work

The main contribution of this paper is to propose a new community-

**Table 7**
Cost and dissatisfaction comparison with baseline for case M in TOU tariffs.

| | | No 5GDHC | Loose penalty | Strong penalty |
|---|---|---|---|---|
| Houses | Bills ($) | 970 | 735 | 745 |
| | Dissatisfaction (person·K$^2$) | 0 | 10,209 | 0 |
| Commercial building | Bills ($) | 270 | 235 | 237 |
| | Dissatisfaction (person·K$^2$) | 0 | 6432 | 0 |
| Data center | Bills ($) | 566 | 74 | 322 |
| | Service reduction (MWh) | 0 | 97.5 | 0 |

based transactive energy market for the 5th generation district heating and cooling systems based on a distributed optimization method. Proximal Jacobian alternating direction method of multipliers (PJ-ADMM) has been used to guarantee the personal privacy of the prosumers while ensuring convergence towards optimal solutions. A market mechanism is proposed to distinguish the allocation of benefits (costs) between prosumers. The market proposed can ensure the budget balance of the coordinator. Furthermore, individual rationality is guaranteed under the constant and TOU electricity rates. The main findings can be summarized as follows:

- The proposed distributed optimization framework provides minimized costs close to those obtained with of a global optimization approach, with differences below 5% for the cases tested. When the number of prosumers is high, a significant reduction of the computational time is also observed.
- The framework allows dynamic management of the thermal demand and internal price to promote heat exchanges between prosumers and reach a balanced network when possible. This dynamic behavior is strongly affected by the electricity tariff structure (constant price, time-of-use, or pay for peak) and can naturally lead to preheating or precooling of the buildings.
- The heat and cold demand profiles of the prosumers strongly affect the dynamic price as well as the heat and cash flows between prosumers. Moving from a heating-dominated to a cooling-dominated network by increasing the size of the data center, the internal price for heat is gradually reduced until it gets negative (which means the data center has to pay to discharge its heat into the network rather than get paid).
- The consumption of electricity was reduced by using the 5GDHC system rather than standalone boilers and chillers in each building. For the cases tested in Section 5.4, the reduction was around 40%. The costs for each prosumer were also less than in the absence of the 5GDCH, thanks to the proposed framework.

As highlighted in this work, the performance and benefits of the proposed framework can vary depending on the demand profiles, which in turn vary depending on the type and number of buildings, weather, tolerance to dissatisfaction, etc. There is thus a need to continue investigating the pros and cons of the system in different contexts. It should also be noted that the capital costs for buying equipment such as heat pumps can also strongly influence the motivations of the coordinator and prosumers to participate in this market. In future work, a long-term market that considers the lifecycle cost can be a relevant topic to study. Finally, a market works well under the assumption of perfect competition. However, in real projects, the market may function badly when there exists a chance for acting "strategically". A market that can achieve a trade-off between privacy protection and incentive compatibility for the 5th generation district heating and cooling systems should be investigated.

## CRediT authorship contribution statement

**Qiwei Qin:** Writing – review & editing, Writing – original draft, Visualization, Validation, Software, Project administration, Methodology, Investigation, Formal analysis, Data curation, Conceptualization. **Louis Gosselin:** Writing – review & editing, Writing – original draft, Visualization, Validation, Supervision, Software, Resources, Project administration, Methodology, Investigation, Funding acquisition, Formal analysis, Data curation, Conceptualization.

## Declaration of competing interest

The authors declare that they have no known competing financial interests or personal relationships that could have appeared to influence the work reported in this paper.

## Data availability

No data was used for the research described in the article.

## Acknowledgments

The authors are grateful to Natural Sciences and Engineering Research Council of Canada for the financial support through its IRC and CRD programs (IRCPJ 461745- 18 and RDCPJ 524504-18) as well as the industrial partners of the NSERC industrial chair on eco-responsible wood construction (CIRCERB).

## Appendix A. Relationship of the internal energy price and the unit cost of the central plant system

The net cost for operating the central plant under the mechanism is:

$$\begin{aligned} min \quad & C_{Central} = \Delta t \sum_{\tau=1}^{24} p_E(t)\dot{E}_{Central}(t) + c_E z_{Central} + \Delta t \sum_{\tau=1}^{24} \lambda(t)\dot{Q}_{net,Central}(t) \\ & = c_E z_B + \Delta t \sum_{\tau=1}^{24} \left\{ \left[ -\lambda(t) + \frac{p_E(t)}{\eta_{Boiler}} \right] \dot{Q}_{Boiler}(t) + \left[ \lambda(t) + \frac{p_E(t)}{COP_{Chiller}} \right] \dot{Q}_{Chiller}(t) \right\} \\ s.t. \quad & \\ & \dot{Q}_{Boiler}(t)\dot{Q}_{Chiller}(t) = 0 \\ & \dot{Q}_{Boiler}(t) \geq 0 \\ & \dot{Q}_{Chiller}(t) \geq 0 \\ & \frac{\dot{Q}_{Boiler}(t)}{\eta_{Boiler}} + \frac{\dot{Q}_{Chiller}(t)}{COP_{Chiller}} \leq z_{Central} \quad for \quad \forall \tau \end{aligned} \tag{31}$$

For constant and TOU electricity rates, $c_E$ is zero and the first order partial derivatives of the boiler's thermal output is:

$$\frac{\partial C_{Central}}{\partial \dot{Q}_{Boiler}(t)} = -\lambda(t) + \frac{p_E(t)}{\eta_{Boiler}} \tag{32}$$

If Eq. (32) is smaller than 0, the optimizer will decide that the thermal output of the boiler is infinite. Then the coordinator will not balance the thermal network and will reduce the price. If the Eq. (32) is larger than 0, the boiler will not be used. In other words, the real time internal thermal price will be the unit cost of the boiler when the boiler is on. For the chiller, a similar situation is found. The internal price will be the unit cost of the chiller when the chiller is on.

For $c_E$ is not zero (C4P tariff), we first rewrite Eq. (31) into the following compact form, and the primal function becomes, $\mathbf{x}$ means the dual variables for the constrains:

$$\begin{aligned} &min \quad C_B = \mathbf{b}^T\mathbf{y} \\ &s.t. \\ &\quad \mathbf{Ay} \geq 0 \quad (\mathbf{x}) \end{aligned} \tag{33}$$

$$\text{where} \quad \mathbf{b} = \begin{bmatrix} \left(-\lambda(1) + \frac{p_E(1)}{\eta_{Boiler}}\right)\Delta t \\ \dots \\ \left(-\lambda(24) + \frac{p_E(24)}{\eta_{Boiler}}\right)\Delta t \\ \left(\lambda(1) + \frac{p_E(1)}{COP_{Chiller}}\right)\Delta t \\ \dots \\ \left(\lambda(24) + \frac{p_E(24)}{COP_{Chiller}}\right)\Delta t \\ c_E \end{bmatrix}, \quad y = \begin{bmatrix} \dot{Q}_{Boiler}(1) \\ \dots \\ \dot{Q}_{Boiler}(24) \\ \dot{Q}_{Chiller}(1) \\ \dots \\ \dot{Q}_{Chiller}(24) \\ z_{Central} \end{bmatrix}, \quad \mathbf{A} = \begin{bmatrix} \mathbf{A_1} & \mathbf{A_2} & & \mathbf{A_4} \\ & \mathbf{A_3} & & \end{bmatrix} \text{with} \mathbf{A_1} = \underbrace{\begin{bmatrix} -\frac{1}{\eta_{Boiler}} & 0 & \dots & 0 \\ 0 & -\frac{1}{\eta_{Boiler}} & \dots & \dots \\ \dots & \dots & \dots & 0 \\ 0 & \dots & 0 & -\frac{1}{\eta_{Boiler}} \end{bmatrix}}_{24rows \times 24columns}, \mathbf{A_2} =$$

$$\underbrace{\begin{bmatrix} -\frac{1}{COP_{Chiller}} & 0 & \dots & 0 \\ 0 & -\frac{1}{COP_{Chiller}} & \dots & \dots \\ \dots & \dots & \dots & 0 \\ 0 & \dots & 0 & -\frac{1}{COP_{Chiller}} \end{bmatrix}}_{24rows \times 24columns}, \mathbf{A_4} = \underbrace{\begin{bmatrix} 1 \\ \dots \\ 1 \end{bmatrix}}_{24rows \times 1column} \quad \text{and } A_3 = \underbrace{[0 \quad \dots \quad 0]}_{1row \times 48columns.}$$

The dual function of the Eq. (33) is:

$$\begin{aligned} &max \quad \mathbf{0}^T\mathbf{x} \\ &s.t. \\ &\quad \mathbf{A}^T\mathbf{x} \leq \mathbf{b} \\ &\quad \mathbf{x} \geq \mathbf{0} \end{aligned} \tag{34}$$

where $\mathbf{x}$ are the dual variables of the constraint in Eq. (33). To make sure there exists feasible solutions of (34), the following condition should be satisfied:

$$\mathbf{A}^T\mathbf{x} \leq \mathbf{b}$$

$$\Leftrightarrow \begin{cases} -\frac{1}{\eta_{Boiler}} x_t \leq \left(-\lambda(t) + \frac{p_E(t)}{\eta_{Boiler}}\right)\Delta t \quad for \quad \forall t = 1, \dots 24 \\ -\frac{1}{COP_{Chiller}} x_{t+24} \leq \left(\lambda(t) + \frac{p_E(t)}{COP_{Chiller}}\right)\Delta t \quad for \quad \forall t = 1, \dots 24 \\ \sum_{t=1}^{49} x_t \leq c_E \end{cases} \tag{35}$$

For constant and TOU price, $c_E = 0$. Therefore, the dual variables $x_t$ are zero. We have:

$$\mathbf{A}^T\mathbf{x} \le \mathbf{b}$$

$$\Leftrightarrow \begin{cases} \lambda(t) \le \dfrac{p_E(t)}{\eta_{Boiler}} \quad for \quad \forall t = 1, \ldots 24 \\ -\dfrac{p_E(t)}{COP_{Chiller}} \le \lambda(t) \quad for \quad \forall t = 1, \ldots 24 \end{cases} \tag{36}$$

That means when extracting heat from the network ($\dot{Q}_{net} > 0$), the price is always equal or smaller than by using the boiler of the central plant. If rejecting heat to the network ($\dot{Q}_{net} < 0$), the price is equal or smaller than by using the chiller of the central plant.

For the charge for peak price, we have:

$$\sum_{t=1}^{24} \lambda(t) \le \frac{1}{\eta_{Boiler}} \sum_{t=1}^{24} \left[ p_E(t) + \frac{x_t}{\Delta t} \right] \le \frac{1}{\eta_{Boiler}} \left[ \sum_{t=1}^{24} p_E(t)\Delta t + \frac{c_E}{\Delta t} \right] \tag{37}$$

$$\sum_{t=1}^{24} \lambda(t) \ge -\frac{1}{COP_{Chiller}} \sum_{\tau=1}^{24} \left[ p_E(t) + \frac{x_{t+24}}{\Delta t} \right] \Big) \ge -\frac{1}{COP_{Chiller}} \left[ \sum_{\tau=1}^{24} p_E(t) + \frac{c_E}{\Delta t} \right] \tag{38}$$

Therefore, for Charge-for-Peak electricity price, the internal price is not guaranteed to be always cheaper than the central plant.

## References


[1] Buffa S, Cozzini M, D'antoni M, Baratieri M, Fedrizzi R. 5th generation district heating and cooling systems: a review of existing cases in Europe. Renew Sustain Energy Rev 2019;104:504–22.
[2] Bünning F, Wetter M, Fuchs M, Müller D. Bidirectional low temperature district energy systems with agent-based control: performance comparison and operation optimization. Appl Energy 2018;209:502–15.
[3] Pellegrini M, Bianchini A. The innovative concept of cold district heating networks: a literature review. Energies 2018;11:236.
[4] Lund H, Østergaard PA, Nielsen TB, Werner S, Thorsen JE, Gudmundsson O, et al. Perspectives on fourth and fifth generation district heating. Energy 2021;227:120520. https://doi.org/10.1016/j.energy.2021.120520.
[5] Project cases | 5GDHC. https://5gdhc.eu/project-cases/; 2024 (accessed May 4, 2024).
[6] Giorgio AD, Liberati F. Near real time load shifting control for residential electricity prosumers under designed and market indexed pricing models. Appl Energy 2014;128:119–32. https://doi.org/10.1016/j.apenergy.2014.04.032.
[7] Brange L, Englund J, Lauenburg P. Prosumers in district heating networks – a Swedish case study. Appl Energy 2016;164:492–500. https://doi.org/10.1016/j.apenergy.2015.12.020.
[8] Nakao M, Nabeshima M, Kobayashi Y, Ishinada M. Thermal grid system and its field test in multiple buildings with individual heating and cooling facility. Energy Procedia 2018;149:112–21.
[9] Wirtz M, Neumaier L, Remmen P, Müller D. Temperature control in 5th generation district heating and cooling networks: an MILP-based operation optimization. Appl Energy 2021;288:116608.
[10] Perfumo C, Kofman E, Braslavsky JH, Ward JK. Load management: model-based control of aggregate power for populations of thermostatically controlled loads. Energ Conver Manage 2012;55:36–48.
[11] Lund H, Østergaard PA, Connolly D, Mathiesen BV. Smart energy and smart energy systems. Energy 2017;137:556–65. https://doi.org/10.1016/j.energy.2017.05.123.
[12] van der Zwan S, Pothof I. Operational optimization of district heating systems with temperature limited sources. Energ Buildings 2020;226:110347. https://doi.org/10.1016/j.enbuild.2020.110347.
[13] Ebeed M, Kamel S, Jurado F. Chapter 7 - Optimal power flow using recent optimization techniques. In: Zobaa AF, Aleem SHEA, Abdelaziz AY, editors. Class. Recent asp. Power Syst. Optim. Academic Press; 2018. p. 157–83. https://doi.org/10.1016/B978-0-12-812441-3.00007-0.
[14] Sameti M, Haghighat F. Optimization approaches in district heating and cooling thermal network. Energ Buildings 2017;140:121–30. https://doi.org/10.1016/j.enbuild.2017.01.062.
[15] Hua W, Sun H, Xiao H, Pei W. Stackelberg game-theoretic strategies for virtual power plant and associated market scheduling under smart grid communication environment. In: 2018 IEEE Int. Conf. Commun. Control Comput. Technol. Smart Grids SmartGridComm. IEEE; 2018. p. 1–6.
[16] Yin S, Ai Q, Li Z, Zhang Y, Lu T. Energy management for aggregate prosumers in a virtual power plant: a robust Stackelberg game approach. Int J Electr Power Energy Syst 2020;117:105605.
[17] Papavasiliou A. Analysis of distribution locational marginal prices. IEEE Trans Smart Grid 2017;9:4872–82.
[18] Boyd S, Parikh N, Chu E, Peleato B, Eckstein J, et al. Distributed optimization and statistical learning via the alternating direction method of multipliers. Found Trends® Mach Learn 2011;3:1–122.
[19] Deng W, Lai M-J, Peng Z, Yin W. Parallel multi-block ADMM with o (1/k) convergence. J Sci Comput 2017;71:712–36.
[20] Lu X, Yu X, Lai J, Wang Y, Guerrero JM. A novel distributed secondary coordination control approach for islanded microgrids. IEEE Trans Smart Grid 2016;9:2726–40.
[21] Liu L, Han Z. Multi-Block ADMM for big data optimization in smart grid. In: 2015 Int. Conf. Comput. Netw. Commun. ICNC, IEEE; 2015. p. 556–61.
[22] Cai H, You S, Wu J. Agent-based distributed demand response in district heating systems. Appl Energy 2020;262:114403.
[23] Mitridati L, Kazempour J, Pinson P. Design and game-theoretic analysis of community-based market mechanisms in heat and electricity systems. Omega 2021;99:102177.
[24] Lund H, Thorsen JE, Jensen SS, Madsen FP. Fourth-generation district heating and motivation tariffs. ASME Open J Eng 2022:1.
[25] Roughgarden T. Algorithmic game theory. Commun ACM 2010;53:78–86.
[26] Bachrach Y, Rosenschein JS. Achieving allocatively-efficient and strongly budget-balanced mechanisms in the network flow domain for bounded-rational agents. In: Agent-Mediat. Electron. Commer. Des. Trading Agents Mech. Springer; 2005. p. 71–84.
[27] Neirotti F, Noussan M, Riverso S, Manganini G. Analysis of different strategies for lowering the operation temperature in existing district heating networks. Energies 2019;12:321.
[28] Vivian J, Emmi G, Zarrella A, Jobard X, Pietruschka D, De Carli M. Evaluating the cost of heat for end users in ultra low temperature district heating networks with booster heat pumps. Energy 2018;153:788–800.
[29] Wyssen I, Gasser L, Wellig B, Meier M. Chiller with small temperature lift for efficient building cooling. Proc Clima 2010;2010.
[30] Ikeda S, Choi W, Ooka R. Optimization method for multiple heat source operation including ground source heat pump considering dynamic variation in ground temperature. Appl Energy 2017;193:466–78.
[31] Olofsson V. 5th Generation District heating and cooling: A high-level simulation model of a Novel District energy network. 2022.
[32] Wang Z, Luo M, Geng Y, Lin B, Zhu Y. A model to compare convective and radiant heating systems for intermittent space heating. Appl Energy 2018;215:211–26.
[33] Wang Z, Chen B, Li H, Hong T. AlphaBuilding ResCommunity: a multi-agent virtual testbed for community-level load coordination. Adv Appl Energy 2021;4:100061.
[34] https://www.energycodes.gov/prototype-building-models. n.d.
[35] Ghatikar G, Piette MA, Fujita S, McKane A, Dudley JH, Radspieler A, et al. Demand response and open automated demand response opportunities for data centers. Berkeley, CA (United States): Lawrence Berkeley National Lab.(LBNL); 2009.
[36] Yu M, Hong SH. Incentive-based demand response considering hierarchical electricity market: a Stackelberg game approach. Appl Energy 2017;203:267–79. https://doi.org/10.1016/j.apenergy.2017.06.010.
[37] Jiang T, Li Z, Jin X, Chen H, Li X, Mu Y. Flexible operation of active distribution network using integrated smart buildings with heating, ventilation and air-conditioning systems. Appl Energy 2018;226:181–96. https://doi.org/10.1016/j.apenergy.2018.05.091.
[38] Nguyen DT, Le LB. Optimal bidding strategy for microgrids considering renewable energy and building thermal dynamics. IEEE Trans Smart Grid 2014;5:1608–20.
[39] Wirtz M, Kivilip L, Remmen P, Müller D. Quantifying demand balancing in bidirectional low temperature networks. Energ Buildings 2020;224:110245. https://doi.org/10.1016/j.enbuild.2020.110245.
[40] https://www.simeb.ca:8443/index_en.jsp. n.d.